52928

School of Pharmacy

Formulation Of Chitosan-Based Nanoparticles For Delivery Of Proteins And Peptides

Vellore Janarthanan Mohanraj

This thesis is presented for the Degree of
Master of Pharmacy
of
Curtin University of Technology

July 2003

ABSTRACT

Delivery of complex molecules such as peptides, proteins, oligonucleotides and plasmids is an intensively studied subject, which has attracted considerable medical and pharmaceutical interest. Encapsulation of these molecules with biodegradable polymers represents one way of overcoming various problems associated with the conventional delivery of macromolecules, for example instability and short biological half-life.

The use of carriers made of hydrophilic polysaccharides such as chitosan, has been pursued as a promising alternative for improving the transport of biologically active macromolecules across biological surfaces. The development of nanoparticles as a delivery system also has major advantages of achieving possible drug protection, controlled release and drug targeting by either a passive or an active means. The aim of this study was to develop a simple and effective method to formulate biodegradable nanoparticles for the delivery of a model protein-bovine serum albumin (BSA) and an angiogenesis inhibitor, arginine-rich hexapeptide (ARH peptide). Major factors which determine nanoparticle formation and loading of the protein and the peptide as well as the underlying mechanisms controlling their incorporation and release characteristics were investigated. The preparation technique, based on the complex coacervation process, is extremely mild and involves the mixture of two aqueous solutions (chitosan and dextran sulfate) at room temperature. The formation of nanoparticles is dependent on the concentrations of chitosan (CS) and dextran sulfate (DS); particles with size, of 257 to 494nm can be obtained with 0.1%w/v solutions of CS and DS. Zeta potential of nanoparticles can be modulated conveniently from -34.3mV to +52.7mV by varying the composition of the two ionic polymers. Both bovine BSA and the ARH peptide were

successfully incorporated into CS-based nanoparticles, mainly via an electrostatic interaction, with entrapment efficiency up to 100% and 75.9% for the protein and peptide respectively. Incorporation of both the protein and peptide into nanoparticles resulted in an increase in size suggesting their close association with the nanoparticle matrix material. The difference in sign and magnitude of zeta potential of empty and macromolecules-loaded nanoparticles supports the hypothesis that protein and peptide association with nanoparticles can be modulated by their ionic interaction with the oppositely charged ionic polymer (DS) in the nanoparticles. The release of BSA from the nanoparticles was very slow in water compared to that in 10mM phosphate buffer pH 7.4; whereas, ARH peptide showed extremely low level of release in water at the low ratio of DS but at the high ratio of DS, its release was in biphasic fashion, with an initial burst effect followed by an almost constant but very slow release up to 7 days in both water and 10mM phosphate buffer (pH 7.4). It was found that, unlike ARH peptide, the percentage of BSA released was relatively slower for the nanoparticles with a high ratio of DS. It is speculated that this difference in the release behaviour of BSA and ARH peptide, could be due to the effect of molecular size of the compounds and their interaction with the polymer matrix of the nanoparticle. The results of this study suggest that these novel CS/DS nanoparticulate system, prepared by a very mild ionic crosslinking technique, have potential to be a suitable carrier for the entrapment and controlled release of peptides and proteins.

ACKNOWLEDGEMENTS

I wish to express my sincere thanks to my supervisor Dr Yan Chen (Lecturer, School of Pharmacy) of Curtin University of Technology for her technical, moral support, patience and advice during progress of this work.

I also thank Associate Professor John Parkin for his valuable guidance as a co-supervisor, Mr. Mike Boddy as a senior technician and John Hess, Information Technology officer, for their assistance in operating analytical, pharmaceutical manufacturing equipment and computer software. Also special thanks to Professor Mike Garlepp for helping me in anyway he could.

I also wish to thank my friends Nivedan, Kavitha, Daryl, Chirag, Anand, and Li Peng for their extensive support during my study.

Finally, I wish to thank all my friends and family back home especially my parents Mr. Janarthanan and Mrs. Varadhal Janarthanan for their great financial support and my wife Gayathri for her continuous moral support, determination and encouragement throughout my study.

Abbreviations

ARH peptide	Arginine-rich hexapeptide
BSA	Bovine serum albumin
CS	Chitosan
DNA	Deoxyribo nucleic acid
DS	Dextran sulfate
GAS	Gas anti-solvent
HPLC	High performance liquid chromatography
HUVE	Human umbilical vein endothelial
IE	Incorporation efficiency
MW	Molecular weight
PACA	Poly alkylcyanoacrylate
PCA	Poly (cyanoacrylate)
PCS	Photon correlation spectroscopy
PEO-PPO	Ethylene oxide-propylene oxide block copolymer
PLA	Poly (lactic acid)
PLG	Poly (D, L-glycolide)
PLGA	Poly (DL-lactide-*co*-glycolide)
RESS	Rapid expansion of supercritical solution
SEM	Scanning electron microphotography
TEM	Transmission electron microscopy
TPP	Tri polyphosphate
VEGF	Vascular endothelial growth factor

Table of Contents

Abstract ii
Abbreviations iv
Acknowledgements v

1. Introduction 3
1.1 The rationale for drug delivery systems 6
1.2 Criteria for an ideal drug delivery system 6
1.3 Sustained and controlled release of drug 8
1.4 Classification of drug carrier systems 9
1.4.1 Particulate carriers 10
1.5 Characteristics of nanoparticles carriers 11
1.6 Limitation of nanoparticles as drug carriers 12
1.7 Preparation of nanoparticles 13
1.7.1 Dispersion of preformed polymers 14
1.7.1.1 Solvent evaporation methods 14
1.7.1.2 Spontaneous emulsification or solvent diffusion methods 14
1.7.1.3 Production of nanoparticles using supercritical fluid technology 15
1.7.2 Polymerization methods 16
1.7.3 Preparation of nanoparticles by coacervation or ionic gelation 17
1.8 Drug loading 17
1.9 Drug release 19
1.10 Particle size 22
1.11 Surface properties of nanoparticles 23
1.11.1 Surface characterization methods 25
1.12 Delivery of peptides and proteins using nanoparticles 26
1.13 Nanoparticulate systems for improved drug delivery 26
1.14 CS and nanoparticles formulation 29
1.15 Dextran sulfate 32
1.16 Arginine-rich hexapeptide 33
1.17 Objective of the study 36
2. Materials and Methods 37
2.1 Materials 37
2.2 Methods 37
2.2.1 Preparation of nanoparticles 38
2.2.1 Incorporation of proteins and peptides into nanoparticles 39
2.2.3 Determination of nanoparticle yield 39
2.2.4 Characterization of chitosan nanoparticles 39
2.2.4.1 Particle size 40
2.2.4.2 Surface properties of nanoparticles 40
2.2.4.3 Morphology of nanoparticles 40
2.2.4.4 Evaluation of the protein loading capacities of nanoparticles 41

2.2.4.5 Evaluation of ARH peptide encapsulation and loading **41**
2.2.4.6 *In-vitro* BSA release from nano-particles **42**
2.2.4.7 *In-vitro* ARH peptide release from nanoparticles **42**
2.2.5 Bradford protein assay **43**
2.2.6 Fluorescence assay of ARH peptide by the fluorescamine derivatization method **44**
2.2.7 Instrumentation of centrifuge **44**
3. Results and Discussion **45**
3.1 Identification of conditions for the formation of CS/DS nanoparticles **46**
3.2 Characterisation of BSA-loaded CS/DS nanoparticles **53**
3.2.1 Particle size and zeta potential **53**
3.2.2 Morphology of empty and BSA-loaded CS/DS nanoparticles **58**
3.2.3 BSA loading and entrapment efficiency **61**
3.2.4 *In Vitro* release of BSA from CS/DS nanoparticles **66**
3.3 Development of a nanoparticle formulation for ARH peptide incorporation. **74**
3.3.1 Preparation of ARH peptide-loaded CS/DS nanoparticles **76**
3.4 Characterisation of ARH peptide-loaded CS/DS nanoparticles **77**
3.4.1 Particle size and zeta potential **77**
3.4.2 Morphology of ARH peptide-loaded nanoparticles **79**
3.4.3 Loading and entrapment efficiency **81**
3.4.4 *In-vitro* release of ARH peptide from CS/DS nanoparticles **85**
4. Conclusions **93**
5. References **95**
6. Appendix **100**

1. Introduction

The most common cause of cancer death in humans is metastasis of the primary tumor to distant sites, not growth of the primary tumor (1). The process of metastasis is aided by many features shared by tumors, including their ability to proliferate at a much faster pace than normal cells (2), their ability to avoid many of the usual adhesion-based control mechanisms for growth and spread, their ability to acquire resistance to a variety of potential chemotherapeutic agents (3) and their ability to form new blood vessels, known as angiogenesis, to enhance their access to necessary nutrients from the host as well as to facilitate their spread into and through the vascular system. Angiogenesis is a significant factor contributing to the distant invasion of cancer cells. This provides access to nourishment for the primary cancer and enables the cells to escape from the tumor and enter the blood stream. Induction of angiogenesis precedes the formation of malignant tumors. Therefore, angiogenesis is a rate-determining step not only for tumor expansion but also for the onset of malignancy.

Numerous angiogenic factors have been identified, but many of these factors possess only very little or no direct mitogenicity on vascular endothelial cells (4). Vascular endothelial growth factor (VEGF) is a specific and potent angiogenic factor and contributes to the development of solid tumors by promoting tumor angiogenesis. Therefore, it is a prime therapeutic target for the development of antagonists for the treatment of cancer. VEGF is a heparin-binding growth factor which has a homodimeric structure and limited sequence homology to the platelet-derived growth factor family and placental growth factor. VEGF is produced in four isoforms having 121, 165, 189, and

209 amino acids possessing heparin-binding domain with the exception of $VEGF_{121}$ and all these isoforms form active disulfide-linked homodimers. Bae and his colleagues (5) identified several arginine-rich peptides from soluble hexapeptide libraries that can inhibit VEGF-induced proliferation of human umbilical vein endothelial (HUVE) cells by direct interaction with VEGF, blocking interaction between $VEGF_{165}$ and $VEGF_{121}$ and the VEGF receptors. The same group also demonstrated that the arginine-rich hexapeptide (ARH peptide: Arginine-Arginine-Lysine-Arginine-Arginine-Arginine, RRKRRR, where R is Arginine and K is Lysine) can block the growth and metastasis of VEGF-secreting HM7 human colon carcinoma cells in nude mice (5). This suggests that the hexapeptide could be useful for the treatments of various angiogenesis-dependent diseases including growth and metastasis of human tumors.

The use of peptides in medicine, however, is generally limited. Their rapid degradation by the proteolytic enzymes in the gastrointestinal tract requires them to be administered through the parentral route. The short biological half-life of peptides also means that they must be administered frequently (6). Furthermore, their poor transportation across biological barriers, caused by poor diffusivity and low partition coefficients often result in a further reduction of their concentration at specific targets. Controlled release parentral dosage forms may be an alternative approach to improve the efficacy of these drugs by reducing the frequency of injection and prolonging the therapeutic plasma level of peptide to eventually increase the concentration of peptide reaching the target. In recent years it has been shown that encapsulating peptides with biodegradable polymers

can improve the delivery of peptides (7). Particulate biodegradable delivery systems have been proposed for the safe and controlled parenteral administration of peptides.

Drug delivery systems such as emulsions, liposomes and nanoparticles, are designed to improve the delivery of drugs to the target sites, while minimizing side effects. The controlled release of pharmacologically active agents to the specific site of action at the therapeutically optimal rate and dose regimen has been a major goal in designing such devices (8). Liposomes have been used as potential drug carriers because of their unique advantages, which include ability to deliver drugs across biological membranes, target drugs to the site of the action and reduce a drug's toxicities or side effects. However, developmental work on liposomes is costly and has been limited due to inherent problems such as low encapsulation efficiency, rapid leakage of water-soluble drug in the presence of blood components and poor storage stability. On the other hand, polymeric nanoparticles offer some specific advantages over liposomes. For instance, they increase the stability of drugs / proteins and possess useful controlled release properties (9, 10).

In the following sections of this introduction, there will be an emphasis on the rationale of delivery systems in cancer therapy regarding controlled release of active agents. It will concentrate on the use of nanoparticles as drug delivery vehicles and highlight the potential and limitations of nanoparticles for drug delivery.

1.1 The rationale for drug delivery systems

The therapeutic effect of a drug in the body comes from its action on "target" macromolecules of the diseased cell; other interactions only result in undesirable or toxic effects of the drug. Because anticancer drugs usually interact with macromolecules shared by a large number of cell types, they generally do more than simply act as toxic agents to the tumour cells and are often associated with serious side effects due to interaction with normal cells. For those drugs which reach the target, chemotherapy can still be compromised due to the problem of incorrect amounts of drug being delivered at improper times. Therefore, drug delivery systems are designed with the rationale of promoting the therapeutic effect of a drug and minimizing its toxic effects. This is achieved by optimizing the amount and duration of the drug in the vicinity of the "target" cell while reducing the drug exposure of "non-target" cells. In short, drug delivery is the use of systems and techniques for spatial and temporal control of drug input to alter the pharmacokinetics and pharmacodynamics of pharmacologically active agents (16).

1.2 Criteria for an ideal drug delivery system

Although individual drug delivery systems may approach the tumour target in different ways and release the drug by different mechanisms, and incorporated anticancer agents can have widely differing properties from one another, it is still possible and necessary to have certain criteria for an ideal drug delivery system to achieve the goal of optimized drug delivery (12). Those criteria for an ideal drug delivery system are:

1. Should be able to incorporate a sufficient amount of active drug and retain biological activity.
2. Should deliver the drug preferentially to tumour cells or enhance the drug effect on those cells and confine the distribution of the drug to a desired site.
3. Should provide a predictable and controllable rate of release.
4. Should release the drug only at its site of action in the body and minimize the leakage of free drug during intravascular transport.
5. Should protect the drug from inactivation by plasma enzymes and undesirable pHs.
6. Should have the capacity to load a wide range of drugs.
7. Should have a suitable size and proper shape to allow carrier system passage to the target site without causing toxicity to the body
8. Should have pharmaceutically acceptable characteristics regarding stability, ease of sterilization, administration, and biodegradability.
9. Should be biocompatible and show negligible antigenicity.

Or in other words, for the nanoparticles to be an ideal drug delivery system they should possess the following properties (13):

1. Selectivity
2. Controlled / sustained release
3. Low immunogenicity
4. Scope of disease
5. Pharmaceutical feasibility

An ideal drug delivery system should be able to transport the drug intact to the sites of action without leakage during transit, drug metabolism or distribution into non-diseased host tissue (selectivity). It should be capable of delivering a therapeutically effective dose to the target sites and release the dose in a controlled manner (controlled / sustained release). It should also be suitable for repeated administration without causing immune responses and hypersensitivity (low immunogenicity). It would be advantageous if many disease types could be treated and different therapeutic agents encapsulated (scope of disease). Finally the formulation has to be practical to produce in bulk and easy to administer to patients (pharmaceutical feasibility).

It is not easy to satisfy all these criteria and so far no single carrier system has done so. However, in order to obtain optimum therapeutic effect, in addition to satisfying the above criteria, one has to consider the mode of action of the drug incorporated into the delivery system and its physiochemical properties so that a proper delivery system can be fabricated and greatest benefit can be derived from incorporation of a drug into the system.

1.3 Sustained and controlled release of drug

Once a drug is accessible to its target, its ultimate therapeutic value depends on its pharmacodynamic effect and the temporal expression of this effect. Therefore, the objective of sustained and controlled drug release is to make a pharmacologically active agent available to a specific target at a rate and a duration designed to accomplish an intended effect.

The advantage of using sustained and controlled drug release systems are:

1. Reproducible and prolonged constant delivery rate.
2. Convenience of less frequent administration.
3. Reduction of fluctuation in circulating drug levels.
4. More uniform effect.
5. Very low dose-related side effects.

Nevertheless, there are also some disadvantages associated with controlled release systems such as high cost and unpredictable and often poor *in vitro* / *in vivo* correlations (14).

Cowsar suggested some general considerations in the design of controlled release systems, which include the need to know or to consider (15):

1. The optimum level of active drug necessary to obtain the desired biological response.
2. The mechanism and rate of active drug removal in the biological environment.
3. The kinetics and mechanism of the delivery of agent from the controlled release system.
4. The influence of the biological environment on the mechanism and kinetics of release.
5. Inherent restriction on the physical and chemical properties of the delivery system materials dictated by the particular application.

1.4 Classification of drug carrier systems

Drug carrier systems for parenteral administration are in general classified into three groups: soluble macromolecular carriers, micellar carriers, and particulate carrier systems.

Due to their difference in physicochemical properties, these three types of system possess distinctive features. Since this study mainly deals with particulate carrier system, in the following sections, characteristics and implications of particulate carrier system will be briefly reviewed.

1.4.1 Particulate carriers

Particulate systems (nano- and microparticles) have been used as a physical approach to alter the pharmacokinetic and pharmacodynamic properties of anticancer drugs. They have been used *in vivo* to protect the drug entity in the systemic circulation, restrict access of the drug to the chosen sites and to deliver the drug at a controlled or sustained release rate to the site of action (16).

Particulate carriers exhibit different mechanisms of distribution, disposition, uptake by the cell and release of the drug when compared to soluble macromolecular carriers (Table 1). There are some advantages of using particulate carriers, which are summarized below (16):

1. Without involving any chemical reaction the drugs can be incorporated into the systems, which can be very important for preserving the drug activity.

2. Drugs can be incorporated chemically, or in the form of macromolecule–drug conjugates, into compartments of the systems. A system of liposome-encapsulated adriamycin-dextran conjugates has been reported which may possess the features of both type of carriers (17).
3. Drug loading can be relatively high.
4. Controlled release characteristics can be readily modulated by the change of matrix constituents.
5. Site-specific targeting of the systems can be achieved by physical means, such as particle size or magnetic guidance (18).
6. Because of their solid form, the movement of carriers is significantly restricted and this confines them to local compartments. This can be useful for chemoembolisation.

Table 1 Comparison the features of soluble macromolecule carriers and particulate carriers

Soluble macromolecule carriers:

(1) Initial distribution is related to the proportion of cardiac output reaching particular organs.
(2) They have the ability to cross endothelial cells of capillaries into interstitial spaces via transcytosis.
(3) They can be taken up by a variety of cell through pinocytosis.
(4) They release coupled drug by dissociation via simple chemical hydrolysis or enzymatic degradation of backbone.

Particulate carriers:

(1) Distribution of the system is non-uniform and mainly determined by the size of particles and vascular anatomy.

(2) Extravasation of the system from the circulation is limited to particles with size < 100 nm, which is only possible through discontinuous endothelia.
(3) They can, in general, only be taken up by the phagocytic cells.
(4) They release drug by the mechanisms of diffusion, dissolution and biodegradation of the matrix.

1.5 Characteristics of nanoparticles carriers

Polymeric nanoparticles, defined as solid particles with a size in the range of 10–1000nm, allow encapsulation of drugs inside a polymeric matrix. Because of their size, the nanoparticles can also be coupled with targeting ligands to provide site-specific delivery, a feature very useful in cancer therapy. The principle of nanoparticles as drug delivery systems is based on the following facts (19):

1. During transit *in vivo* they prevent the degradation and retard the release of the drug by minimizing the interaction of loaded drug with blood components.
2. They control and sustain release of the drug during the transportation and at the site of localization, altering organ distribution of the drug. Thus, subsequent clearance of the drug can be manipulated so as to achieve a reduction in undesired side effects and increase in drug therapeutic efficacy.
3. Their particle size and surface characteristics can be manipulated to achieve both passive and active drug targeting after parenteral administration.
4. They can be used as long-acting depot preparations.

1.6 Limitation of nanoparticles as drug carriers

Though the polymeric nanoparticles offer some specific advantages over other carrier systems, they do have some limitations, for example, their small size and large surface tension can lead to particle-particle aggregation, making physical handling of nanoparticles difficult in liquid and dry powder forms. This is a practical problem that has to be overcome before nanoparticles can be used clinically or commercially drug delivery. It is also found that the nanoparticles have shown to be very effective for the sustained release of drugs into the periodontal pocket, with an ability to penetrate intact and deep into regions which are probably inaccessible for other devices. Their use, however, as carriers is much limited due to the preparation methods, which allowed only the encapsulation of poorly or non-soluble water drugs. Hence, more studies are needed to determine the usefulness of biodegradable nanoparticles as an intra-pocket carrier system (20).

1.7 Preparation of nanoparticles

Nanoparticles can be prepared from a variety of materials such as proteins, polysaccharides and synthetic polymers. The selection of matrix material is dependent on many factors (21):

1. Size of nanoparticles required.
2. Inherent properties of the drug for example, aqueous solubility and stability.
3. Surface characteristics of particles such as permeability and charge.
4. Degree of biodegradability, biocompatibility and toxicity.
5. Drug release profile desired.

6. The antigenicity of the final product.

Nanoparticles are generally prepared by three methods, depending upon the nature of matrix materials selected, dispersion of the pre-formed polymers, polymerization of monomers and coacervation.

1.7.1 Dispersion of preformed polymers

Several methods have been used to prepare biodegradable nanoparticles from poly (lactic acid) PLA, poly (DL-glycolide) PLG, poly (D,L-lactide-*co*-glycolide) PLGA, and poly (cyanoacrylate) PCA, by dispersing preformed polymers.

1.7.1.1 Solvent evaporation methods

In this method, the polymer is dissolved in an organic solvent such as dichloromethane, chloroform or ethyl acetate and the drug is dissolved or dispersed in the polymer solution. The mixture is then emulsified into an aqueous solution to make an oil-in-water (O/W) emulsion by using a surfactant or emulsifying agent. After the formation of a stable emulsion, the organic solvent is evaporated either by increasing the temperature under reduced pressure or by continuous stirring. This method involves high-speed homogenization or sonication process (22).

1.7.1.2 Spontaneous emulsification or solvent diffusion methods

This is a modified version of the solvent evaporation method in which the water-soluble solvent along with the water insoluble organic solvent is used as an oil phase. Due to the spontaneous diffusion an interfacial turbulence is created between the two phases leading

to the formation of small particles (23). A considerable decrease in particle size is achieved as the concentration of water-soluble solvent increases.

1.7.1.3 Production of nanoparticles using supercritical fluid technology

Conventional methods like solvent evaporation, coacervation and polymerization often require the use of toxic solvents or surfactants. Hence research efforts have been directed to develop environmentally safer encapsulation methods to produce the drug-loaded nanoparticles because the solvent impurities remaining in the drug loaded particles increase toxicity. It may also degrade the pharmaceuticals within the polymer matrix. In order to overcome this problem supercritical fluids have been proposed. This is found to be an attractive alternative as these are environmentally friendly solvents and the method can be used to process particles to high purity without any trace amount of organic solvent.

In the rapid expansion of supercritical solution (RESS) method the solute of interest is solubilized in a supercritical fluid and the solution is expanded through a nozzle. Thus, the solvent power of supercritical fluids dramatically decreases and the solute eventually precipitates. This technique is clean because the precipitated solute is completely solvent-free. Unfortunately, most polymers exhibit little or no solubility in supercritical fluids making the technique less of practical interest (24). This method is useful for low molecular weight polymers (< 10,000 daltons) as matrix materials and can achieve uniform distribution of drug inside the polymer matrix but high molecular weight polymers cannot be used due to their limited solubility in supercritical fluids (25).

In the supercritical anti-solvent (SAS) method, the solution is charged with the supercritical fluid in the precipitation vessel containing solute of interest in an organic solvent. At high pressure, enough anti-solvent will enter into the liquid phases so that the solvent power will be lowered and the solute precipitates. After precipitation, when the final operating pressure is reached, the anti-solvent flows through the vessel so as to strip the residual solvent. When the solvent content is reduced to the desired level, the vessel is depressurized and the solid product is collected. This method, also called the gas anti-solvent (GAS) technique, has been successfully used to produce nanoparticles (26).

1.7.2 Polymerization methods

Nanoparticles can also be prepared by polymerization of monomers. In this technique, a drug is dissolved in the polymerization medium either before the addition of the monomer or at the end of the polymerization reaction. The nanoparticle suspension is then purified by ultra centrifugation or by re-suspending the particles in an isotonic surfactant-free medium (27). During polymerization various stabilizers and surfactants are also used. Particle size and molecular mass of nanoparticles depend upon the type and concentration of stabilizer and surfactant used. Polyalkylcyanoacrylate (PACA) nanoparticles are typically prepared using this method to improve the therapeutic activity of drugs, mainly antineoplastics and antibiotics. Couvreur et al. reported the production of polycyanoacrylate nanoparticles (200 nm diameter) by mechanically polymerizing the dispersed methyl or ethyl cyanoacrylate acidic medium in the presence of the surfactant polysorbate-20 without irradiation or an initiator (27).

1.7.3 Preparation of nanoparticles by coacervation or ionic gelation

Much research is now focused on the preparation of nanoparticles using biodegradable hydrophilic polymers such as CS, gelatin and sodium alginate. Different methods are adopted to prepare nanoparticles from these hydrophilic polymers. Calvo and coworkers have reported preparing hydrophilic CS nanoparticles by ionic gelation (28). The method involves a mixture of two aqueous phases, of which one is the polymer CS and a diblock copolymer of ethylene oxide and propylene oxide (PEO-PPO) and the other is a polyanion sodium tripolyphosphate (TPP). In this method, the positively charged amino group of CS interacts with the negatively charged TPP to form coacervates with sizes in the nanometer range. These nanoparticles have good association with proteins, and their size (200-1000 nm) and zeta potential (between +20 mV and +60 mV) can be modulated by varying the ratio of CS/PEO-PPO (29).

Some workers have adopted a similar approach, using the complex coacervation process to prepare nanoparticles from hydrophilic polymers (30). It is a spontaneous phase separation process that occurs when oppositely charged macromolecules are mixed. It is a result of electrostatic interaction and coacervates form under mild conditions, whereas, ionic gelation involves the material undergoing transition from liquid to gel due to ionic interaction under conditions of controlled temperature.

1.8 Drug loading

Ideally, a successful nanoparticle system should have a high drug loading capacity, thereby reducing the quantity of matrix materials required for administration.

Incorporation of drug into the nanoparticles can be achieved by two methods: one, by incorporating the drug at the time of nanoparticle production or secondly, by absorbing the drug after the formation of nanoparticles by incubating the carrier with the drug solution. It is evident that potentially a larger amount of drug can be entrapped by the incorporation method when compared with the adsorption / absorption technique (31). Adsorption isotherms of drug to nanoparticle system give vital information on the best possible formulation, the drug binding capacity onto the surface of nanoparticles and the amount of drug absorbed. In some studies it is seen that the capacity of adsorption / absorption is also related to the hydrophobicity of the polymer and the specific area of the nanoparticles (31). In the case of the entrapment method for nanoparticles prepared by polymerization technique, it is found that an increase in concentration of the monomer increases the association of drug whereas a reverse trend is observed with the drug concentration in the dispersed solution. This was further supported by the studies on the effect of monomer concentration on percentage drug loading. Hence, these results indicate that it is important to optimize the amount of monomer available for drug entrapment. Also, the type of surface–active materials and stabilizers has an effect on drug loading. In addition to the above-mentioned methods of drug loading, an alternative method, in which the drug is chemically conjugated into nanoparticles has been proposed (32).

Preparation of CS nanoparticles under mild conditions by coacervation techniques, appears to be a very effective way for the association and delivery of sensitive macromolecules such as BSA, tetanus toxoid, and insulin. The ability of CS nanoparticles

to encapsulate these molecules was so high that, to obtain a desired final protein loading, all that was required was to adjust the amount of protein added to the formulation (33). Protein association studies of CS nanoparticles carried out at different pH values indicate that, for a particular protein, the greatest loading efficiency is obtained when the protein is dissolved at a pH above its iso-electric point, so that the macromolecule is predominantly negatively charged. It is also found that the post loading of protein does have a significant effect on the entrapment efficiency in that a significantly smaller amount of protein is found to be incorporated into a previously formed nanoparticle suspension (28). This could be due to the reduced number of amino groups on CS available in nanoparticles, after its interaction with polyanions, for interaction with negatively charged protein.

1.9 Drug release

Drug release from nanoparticles and subsequent biodegradation are important for developing successful formulations.

The release rates achieved depend on the following:

(1) Solubility of drug.

(2) Desorption of the surface-bound/adsorbed drug.

(3) Drug diffusion through the nanoparticle matrix.

(4) Nanoparticle matrix erosion.

(5) A combination of erosion/diffusion process.

Thus, solubility, diffusion and biodegradation of the matrix materials govern the process of drug release.

The various methods (34) to study the *in vitro* release are:

1. Side-by-side diffusion cells with artificial or biological membranes.
2. Dialysis bag diffusion techniques.
3. Reverse dialysis sac techniques.
4. Agitation followed by ultra-centrifugation/centrifugation.
5. Ultra-filtration or centrifugal ultra-filtration techniques.

The release study is often performed by a method of controlled agitation followed by centrifugation. Due to some technical difficulties in separation of nanoparticles from release media, which sometimes can be tedious and time-consuming, a number of *in vitro* release studies of nanoparticles, have been conducted by dialysis techniques now (35). In some studies reverse dialysis techniques are used by dispersing nanoparticles directly into the dissolution medium but this is normally for formulations having release of more than an hour (36).

Release profiles of the drugs from nanoparticles depend on the nature of the delivery system used and the interactions between the drug and matrix materials. In the case of a matrix device where a drug is uniformly distributed or dissolved in the matrix, the release occurs predominately by diffusion and or erosion of the matrix under sink conditions. If the diffusion of the drug is faster than matrix degradation, then the mechanism of drug release is controlled by the diffusion process (drug loading, particle size / surface area, drug solubility etc are the controlling factors), otherwise it depends upon degradation or both. The rapid initial release (i.e. burst release) of drug is mainly attributed to the fraction of drug which is adsorbed or weakly bound to the large surface area of the nanoparticles, rather than due to the release of drug incorporated in nanoparticles.

The method of drug incorporation into nanoparticles has also been shown to have an effect on drug release. It has been reported that the nanoparticles loaded with drug by incorporation methods show less burst effect and better sustained release characteristics than that produced by adsorption methods which demonstrate higher burst effects of up to 60-70% of the drug, due to the fact that, in the latter, a higher proportion of drug is weakly associated with the matrix of nanoparticles and less involved in ionic or hydrophobic interactions with the polymer matrix (37).

Polakovic et al. used two models to study the release of lidocaine from nanoparticles (38):

(1) By crystal dissolution.

(2) By diffusion through the polymer matrix.

They found that when the drug loading was less than 10% (w/w), the release kinetics showed a better fit to the diffusion model, whereas at concentrations greater than 10% lidocaine crystals were observed. The drug dissolved firstly from the crystals and then had to diffuse through the matrix; hence the overall release mechanism could be described by the dissolution model.

Calvo et al. obtained release profiles of indomethacin, exhibiting zero-order kinetics from both nanoparticles and nanocapsules coated with the polymer, which occurred by diffusion of the drug from the core across the polymeric barrier layer (10). The study indicated that the polymer coating acts as a barrier to the release of the drug, mainly

caused by the partitioning of the drug between the polymer and release medium. The main factor controlling the release is the volume of the aqueous media, the higher the dilution of the dissolution media, the faster and more complete the release of drug (10). Yoo et al. reported that when the drug was chemically conjugated with PLGA in nanoparticles, the release took place over 25 days, whereas with nanoparticles containing unconjugated free drug, a rapid and complete release occurred in 5 days (32). Here, the controlled release properties of the drug have been attributed to chemical degradation of the conjugated PLGA, which permitted solubilization and subsequent release of the drug-conjugated PLGA oligomers into the medium. In the case of hydrogel nanoparticles, the release is related to swelling, which can be controlled by either modulating the hydrophilic functional groups or by monitoring cross-linking of the matrix (32).

The *in vitro* release behavior of ionically cross-linked nanoparticles was also found to be affected by the addition of auxiliary ingredients in the nanoparticles. Calvo et al. reported a significant increase in the release rate of BSA when PEO-PPO was incorporated into the nanoparticles (29). This difference in the release rate could be attributed to the reduced interaction between BSA and CS, due to the presence of PEO-PPO, or to the lower BSA loading of the nanoparticles. In addition, in CS nanoparticles containing different BSA loadings, the percentage of BSA released over time was higher for those formulations containing a lower protein loading (29). These results demonstrate that the release characteristics of the proteins can be modulated simply by adjusting the composition of CS nanoparticles or their protein loading.

1.10 Particle size

The size of nanoparticles is of importance in determining the performance of nanoparticulate systems *in vitro* as well as the therapeutic effect of the incorporated drug. The particle size of the nanoparticles influences the release rate and potentially the *in vivo* distribution of nanoparticles. Their size was very much affected by their preparation conditions. Large particles have a relatively smaller surface area compared to the small particles with the same total volume; therefore most of the associated drug won't be at or near the particle surface and cannot be readily released. Furthermore, the diffusion distances encountered in large particles are greater which allows drug trapped in the core to slowly diffuse out and also for the release medium to slowly diffuse in (40). Therefore, a study of the size of nanoparticles is an important step in design and development of this system in order to optimize their performance.

1.11 Surface properties of nanoparticles

Surface properties including surface charge and surface hydrophilicity/hydrophobicity are important factors determining nanoparticles dispersion *in vitro* and their biological fate. When nanoparticles are administered intravenously, they are recognized readily by the bodies' immune system and then cleared from the circulation (35). Apart from the size of nanoparticles, their surface hydrophobicity determines the amount of adsorbed blood components, mainly proteins (opsonins). The opsonised particles are then taken up by phagocytes, as the part of the body defense system to remove foreign substances. To avoid this *in vivo* fate, the surface of nanoparticles is often modified with a hydrophilic polymer, which acts as a shield between nanoparticles and opsonins. Hence, for a

qualitative and quantitative understanding of the interaction of blood proteins with nanoparticles, it is necessary to design long-circulating nanoparticles by surface modification. The surface properties of nanoparticles, their plasma protein adsorption and phagocytosis of nanoparticles have been widely studied (39, 40).

The surface charge of the nanoparticles is determined by the electrostatic properties of the polymer. When the neutral polymer is applied, the surface charge of nanoparticles is usually neutral or slightly negative, whereas, when a cationic polymer is applied, the zeta potential of nanoparticles is positive.

When administered intravenously, nanoparticles coated with hydrophobic polymers tend to be easily captured by lymphatic cells in the body, because the particle, which has a hydrophobic surface, is usually recognized more readily by opsonins. However, when poloxomers are used as the surfactants during the preparation process, they were effectively adsorbed onto the surface of nanoparticles to form a hydrophilic layer, which prevents the approach of opsonins. This phenomenon can be directly detected by determining the increment of diameter after the addition of surfactant solution into the nanoparticles solution. It was also confirmed that the nanoparticles coated with a hydrophilic layer tend to provide a longer systemic circulation when intravenously administered, as was generally recognized (39). Carboxylated poly (styrene) nanoparticles show a significantly decreased affinity to intestinal epithelia, especially to M cells, compared to positively charged and uncharged poly (styrene) nanoparticles (41). On the other hand, nanoparticles consisting of negatively charged poly (anhydride)

copolymers of fumaric and sebacic acid, show greatly increased particle adhesion to the cell surfaces (42). These results support the hypothesis that the uncharged and positively charged nanoparticles consisting of hydrophobic poly (styrene) provide an affinity to absorptive enterocytes, whereas, negatively charged nanoparticles from more hydrophilic polymers show highly increased bioadhesive properties and are adsorbed by both M cells and absorptive enterocytes. This also showed that a combination of both nanoparticles surface charges and increased hydrophilicity of the matrix material were responsible for the gastrointestinal uptake of the nanoparticles.

1.11.1 Surface characterization methods

Surface properties of particles can be measured by estimating the surface charge, density of the functional groups or surface hydrophilicity. Zeta potential is one of the methods by which the mobility of charged particles in an applied electrical field is monitored. This practical surface potential may be either positive or negative depending upon the nature of polymer or material used for preparation of nanoparticle or subsequent surface treatment and the presence of oppositely charged ionic substances. The other method used to characterize the surface is x-ray photoelectron spectroscopy, which is based on the emission of electrons from materials in response to irradiation by photons of sufficient energy to cause ionization of core-level electrons. These electrons are emitted at energies characteristic of the atoms from which they are emitted. By this technique surface elemental analysis can be performed (43). In another technique, the surface hydrophobicity of nanoparticles is directly measured by hydrophobic interaction chromatography, in which the column chromatography is used to separate the materials based on the interaction with a hydrophobic gel matrix (44).

1.12 Delivery of peptides and proteins using nanoparticles

Peptide and protein drugs are of interest because of their roles in physiopathology and the progress being made in biotechnology and bioengineering. Their use in medicine is partly limited due to their rapid degradation by proteolytic enzymes in the gastrointestinal tract which necessitates them being administered via the parenteral route. The biological half-life of peptides is short and they require frequent administration. In addition, their transport across biological barriers is poor due to poor diffusivity and lower partition coefficients, often resulting in further reduction of their concentration at the specific target. Controlled release parenteral dosage forms may be an alternative approach to improve the efficacy of these drugs by reducing the frequency of injections and prolong therapeutic plasma level of peptide to eventually increase the concentration of peptide reaching the target. It has been shown that encapsulating peptides with biodegradable polymers can improve the delivery of peptides. Particulate biodegradable delivery systems like nanoparticles are developed for the safe and controlled administration of peptides (45).

1.13 Nanoparticulate systems for improved drug delivery

Recent advances in nanoparticulate systems show their promise as potential ideal drug delivery systems for poorly soluble, poorly absorbed and labile substances (46). It's been found that the use of nanoparticulate formulation and highly soluble excipients can increase solubility and dissolution rate of poorly soluble substances for oral dosage forms, due to nanosizing, which is a promising way for improving drug bioavailability.

For example, nanosized dispersed solid particles called nanosuspensions, developed using a high-pressure homogenizer, results in excellent adhesion to biological surfaces (e.g. the epithelial gut wall) as well as increasing the solubility and dissolution rate. In addition, nanoparticulate systems with controlled release properties were also found capable of targeting drug to the brain and bone marrow following intravenous injection (47).

Nanoparticulate systems offer protection for the drug molecules, which are unstable physicochemically, or biochemically in a particular environment. This is because in polymeric nanoparticulate systems, drug molecules can be encapsulated in the form of a solid solution or dispersion or be chemically bound. Such a drug-polymer hybrid or combined system offers the loaded drug more delivery properties. The properties such as particle size and distribution, surface charge, and hydrophilicity determine the functions and performance of nanoparticles, which can also be modified by selecting appropriate polymer materials. It is these properties of nanoparticles and to a lesser extent of intrinsic physicochemical properties of drug molecules, which determine the biological performance or therapeutic efficacy of the drug.

A new chemical approach for preparation of nanoparticles/nanospheres, composed of novel graft copolymers, has been studied for oral peptide delivery. It involves mucoadhesive PLGA nanoparticles/nanospheres prepared by the emulsion solvent diffusion process followed by surface modification with mucoadhesive polymer such as CS and acrylic polymer. It was found that this system provides enhanced oral absorption of peptides, due to improved drug retention and stability (47). This mucoadhesive

nanoparticulate system with peptide drugs could significantly improve and prolong the biological action of the enclosed drugs following oral administration.

Another characteristic function of nanoparticles/nanospheres is their ability to deliver the drug across a number of biological barriers to the target site. Lymphatic targeting of drugs has been achieved using polyisobutyl-cyanoacrylate nanoparticles/nanospheres with a suitable size distribution and appropriate surface characteristics to enhance the accumulation of drug in lymph nodes following oral administration (47).

The delivery of a wide variety of drugs such as central nervous system-active agents, antineoplastics and antibiotics to the brain is hindered because of the difficulty drugs have in crossing the blood-brain barrier. The application of nanoparticles/nanospheres to brain delivery is found to be a promising way to overcome this barrier. It has been found that polysorbate80-coated nanoparticles/nanospheres are capable of transporting the hexapeptide dalargin, the dipeptide kytorphin, doxorubicin and the other agents into the brain after intravenous administration (48).

CS nanoparticles have been extensively studied as a carrier for transporting the associated therapeutic molecules such as proteins, peptides and oligonucleotides through the different types of mucosae and epithelia [49]. It has also been found that DNA-CS hybrid nanoparticles/nanospheres are effective transfection carriers.

All these show that nanoparticulate systems have great potential and ability to convert poorly soluble, poorly absorbed and labile biologically active substances into promising drugs. The choice of polymer as a matrix material is very important as these materials, once administered in the form of nanoparticles, are in direct contact with our biological

system and their biocompatibility, biodegradability and non-toxicity should be considered.

1.14 CS and nanoparticles formulation

CS is derived from chitin, nature's second most abundant polymer after cellulose. CS is generally produced from crustaceans, with the parent biomass being primarily crab and prawn shells. However, CS may also be derived from fungal chitins. Structurally, CS is a polysaccharide, derived by deacetylation of chitin (50). Chemically, CS is polymer of α(1-4)-2-amino-2-deoxy-D-glucose (D-N-glucosamine) residues (See Figure 1).

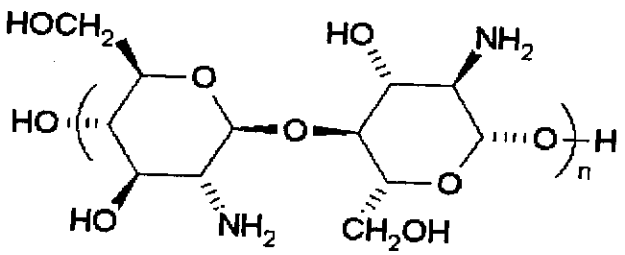

Figure 1 Structure of CS

Even though the discovery of CS dates back to the nineteenth century, it has only been over the last two decades that this polymer has received attention as a material for biomedical and drug delivery applications. The accumulated information about the physicochemical and biological properties of CS led to the recognition of this polymer as a promising material for drug delivery and, more specifically, for the delivery of delicate macromolecules (51, 52). From a technical point of view, it is extremely important that CS is water soluble and positively charged. These properties enable it to interact with negatively charged polymers, macromolecules, and even with certain polyanions on contact in an aqueous environment. These interactive forces and sol-gel transition stages

can be exploited for nano-encapsulation purposes. From a biopharmaceutical point of view, CS has a special feature of adhering to mucosal surfaces (53), a fact that makes it useful polymer for mucosal drug delivery (54). The potential of CS for this specific application has been further reinforced by the demonstrated binding capacity of CS to open tight junctions between epithelial cells thus facilitating the transport of macromolecules through well organized epithelia (55). The interesting biopharmaceutical characteristics of this polymer are accompanied by its well-documented important properties such as mucoadhesivity, biocompatibility and low cytotoxicity (56).

CS is available in different forms such as CS hydrochloride, CS hydroglutamate, glycol CS and CS hydro lactate with varying molecular weights and degrees of acetylation. It has been found that polymers of high molecular weight of each type of CS were most toxic (57). The ranking of cytotoxicity of different salts of CS and their derivative are: CS hydrochloride > CS hydroglutamate > glycol CS > CS hydro lactate. Investigation on CS's degree of deacetylation and molecular weight showed that a high degree of deacetylation are effective as permeation enhancers at low and high molecular weight and also reveal clear dose-dependent toxicity, whereas CS of low degree of deacetylation were effective at only high molecular weight and show low toxicity. The effects of CS's of both high and low molecular weight and degree of deacetylation were further investigated as regards their ability to bind at epithelial Caco-2 cell monolayers. Both CSs appeared to bind tightly to epithelia and no intracellular uptake of CS was observed, showing that these effects were mediated by CS's cationic charges (57).

The solubility of polysaccharide CS is very poor. This is the main reason why this natural polymer cannot be degraded effectively. However, the amino group at the C-2 position of the sugar ring leads to a unique intrinsic property of CS in terms of solubility in aqueous solution. At lower pH (<5), the amino groups on the polysaccharides are extensively protonated, resulting in a strong solvolysis of the polymer chain with water molecules. Whereas, at pH >7.0, the solubility of CS decreases considerably limiting its use as an absorption enhancer in, for example, nasal or peroral delivery systems (58). To overcome this problem, a number of cationic and anionic CS derivatives have been synthesized and tested. Particles prepared from CS beads also showed a pH-dependent swelling and solubilising behavior, which makes them appropriate for the delivery of drugs in the gastric cavity or to acidic, compartments such as endosome or lysosome (59, 60). The latter is a quality that may give advantages to these nanoparticles in the field of gene therapy (61).

CS nanoparticles can be prepared by a number of methods, which are classified into two main categories depending on whether the polymer is formed by a polymerization reaction or by a physicochemical process, such as pressure homogenization, emulsification, precipitation or polymeric spherical crystallization using a macromolecule directly or a preformed polymer. Recently, the use of complexation between oppositely charged macromolecules to prepare CS nanoparticles as a controlled release formulation, especially for peptide and protein drug delivery, has attracted much attention, because this process is very simple and mild (28). CS nanoparticles were obtained spontaneously under constant magnetic stirring at room temperature on addition of tripolyphosphate to

CS solution due to ionic gelation. In addition, this process involves reversible physical cross-linking by electrostatic interaction, which possibly avoids toxicity of reagents and other undesirable effects. It also has great potential for the encapsulation of living cells and labile molecules, which are unable to withstand harsh conditions (heat, organic solvents) involved in other encapsulation process. This is also the basis for choosing CS as the matrix material in this study.

1.15 Dextran Sulfate (DS)

DS is a polyanion similar to heparin with a branched carbohydrate backbone and negatively charged sulfate groups. DS used in this study was derived from leuconostoc mesenteroides, strain B512 and contains approximately 17% sulfur, which is equivalent to approximately 2.3 sulfate groups per glucosyl residue.

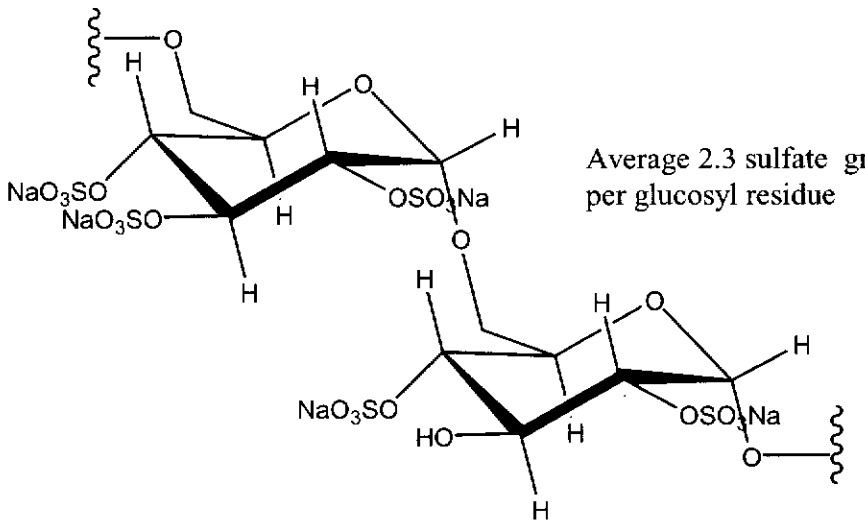

Figure 2 Structure of DS sodium

In low ionic strength solutions the DS polymer will be fully extended due to repulsion of the negatively charged sulfate groups, whereas, in high ionic strength solutions the polymer shrinks and more closely resembles unionized dextran.

In recent years DS has found many applications in biomedical and biotechnology research away from lipoprotein separation. It is used in the isolation of ribosomes and to release DNA from histone complexes. It can also promote hybridization of probes with DNA and complexes with fibrinogen. It has also been reported as an effective matrix material for controlling release of basic drugs such as doxorubicin on the basis of ionic interaction (62).

1.16 Arginine-rich hexapeptide

ARH peptide was first identified by Bae and his colleagues (5) from soluble hexapeptide libraries. It was found capable of blocking the growth and metastasis of VEGF-secreting HM7 human colon carcinoma cells in nude mice. Furthermore, the ARH peptide showed significant inhibition of angiogenesis induced by VEGF in the chorioallantoic membrane and the rabbit cornea neovascularization assays. This suggests that the ARH peptide which can inhibit angiogenesis could be useful for the treatments of various angiogenesis-dependent diseases including growth and metastasis of human tumors. Potentially it could serve as a lead compound for development of more effective anti-angiogenic molecules. The development of appropriate vehicles to deliver this new macromolecule was a great challenge, as we know the peptides are very unstable compounds that need to be protected from degradation in the biological environment.

Moreover, their efficacy is highly limited by their ability to cross biological barriers and reach the target site. As such, the future of these molecules as therapeutic agents clearly depends on the design of an appropriate vehicle for their delivery to the body. Several strategies have been explored among which the design of biodegradable nanoparticles using CS has drawn considerable interest and found to be promising for the association and delivery of labile macromolecular compounds. As particulate drug delivery systems have been shown to influence the pharmacokinetics of drug molecules in the body, a nanoparticulate system was chosen to provide the controlled delivery of the peptide of interest (i.e. ARH peptide). We are interested in developing CS nanoparticles for incorporation of this ARH peptide to achieve sustained release purpose.

Structure of Arginine (Arg)

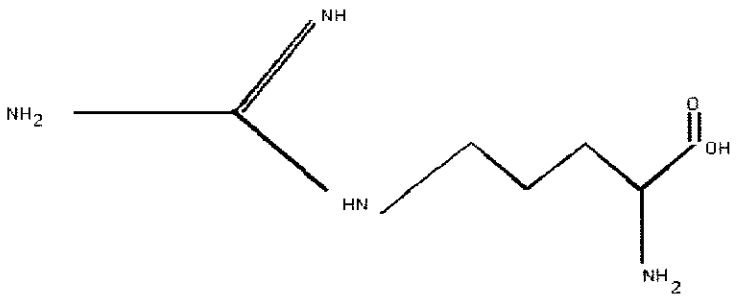

Structure of Lysine (Lys)

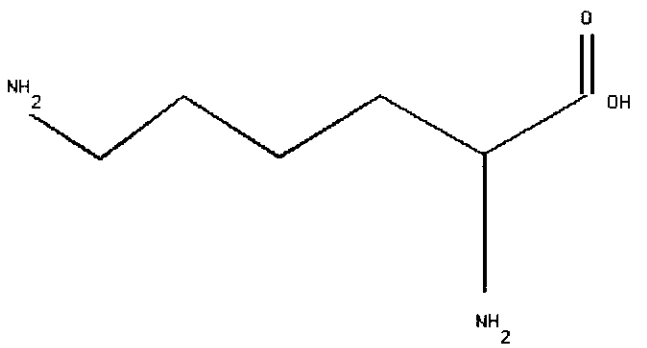

Figure 3 Structure of arginine and lysine

1.17 Objective of the study

The objective of this work was to develop a new type of hydrophilic nanoparticle, based on the method developed by Calvo et al. (29), for sustained delivery of protein and peptide and to evaluate nanoparticle properties in relation to the entrapment and controlled release of proteins and peptides. We chose to use the hydrophilic polymer CS and poly-anion DS for the preparation of the nanoparticles by complex coacervation process. The peptide and protein may be physically trapped, adsorbed into nanoparticles or associated with the polymer matrix via ionic interaction. Obviously, *in vivo*, the drug would have to be released by diffusion, desorption, ion exchange or hydrolysis/degradation of the matrix materials.

The combination of the polymer CS with DS was evaluated as matrix materials for hydrophilic nanoparticles with the objective to understanding how the ratio of opposite charged matrix material may affect the characteristics of nanoparticles, e.g. size, charge, drug loading and release. In this study, BSA was used initially as a model protein instead of ARH peptide to optimize the preparation conditions in the initial stage because of the high cost of the ARH peptide. The use of BSA as a model drug also allowed us to compare the entrapment and controlled release of a large and a small molecule by the hydrophilic CS nanoparticles. The knowledge and information obtained from this study will give us a better understanding of the formulation for both large and small molecules of protein and peptide, using hydrophilic polymers.

2. Materials and Methods

2.1 Materials

The polymer CS (medium molecular weight: 400,000 and Catalog no: 22742) was purchased from Fluka / Sigma-Aldrich, Australia. ARH peptide (Mw: 927, code no: CS and Batch no: M10384, Purity 95%) was synthesized by Auspep Pty Ltd, Australia. BSA (Fraction V, Code no: A-7906); sodium salt of DS (Mw: 10,000 and Catalog no: D6924), sodium phosphate dibasic (Mw: 141.96); Bradford reagent (Fraction Code no: B-6916) and fluorescamine (Code no: F-9015) were purchased from Sigma Chemical Co. (St. Louis, Missouri, USA). Fluorescamine was dissolved in HPLC-grade acetonitrile. All other solvents and materials were of analytical grade. Deionized water (Milli-Q water) was used in the preparation of buffers and standard solutions of peptide. Chemicals and reagents used in this research if not specified were all used as received.

2.2 Method

2.2.1 Preparation of nanoparticles

The hydrophilic nanoparticles were prepared using the complex coacervation of CS and DS. This is a modification of the method reported by Calvo et al. (29). Specifically, a polysaccharide CS solution and a solution containing the polyanion DS were mixed at room temperature under magnetic stirring to produce nanoparticles. CS and DS, when mixed, undergo a coacervation process, as a result of ionic interactions. Nanoparticles are formed under mild conditions.

To prepare CS solutions, various amounts of CS were dissolved in aqueous acetic acid to obtain final CS concentrations of 0.1%, 0.25%, 0.5% and 1%(w/v) .The concentration of

acetic acid was 1.75 times higher than that of CS in all cases. DS was dissolved in purified water at the same concentration as CS (0.1%, 0.25%, 0.5% and 1%w/v). Finally, variable volumes of the DS solution (1, 2, 3, 4, 5, 8.5 and 10mL) were added to 5mL of the CS solution with magnetic stirring (speed level 6 using an IEC magnetic stirrer) at room temperature for 15 minutes. The pH of solutions was then measured and correlated to the formation of nanoparticles. All samples were microscopically examined, sized by the method described in section 2.2.4.1 and then classified according to their size.

The ratio, which produced the highest yield of desirable nanoparticles of suitable size and large negative charge, was used as the method of choice for preparation of nanoparticles for loading both BSA and therapeutic ARH peptide.

2.2.2 Incorporation of proteins and peptides into nanoparticles

Incorporation of the BSA into the nanoparticles was performed by dissolving BSA in either the polycation CS or in polyanion DS to obtain a BSA concentration of 1mg/mL in the polymer before mixing with oppositely charged polymer. The BSA-loaded nanoparticles were formed spontaneously upon addition of variable volume of 3mL, 5mL, and 8.5mL (0.1% w/w) of the DS aqueous solution to 5ml of the CS acidic solution (0.1% w/w) with magnetic stirring for 15 minutes. The ARH peptide-loaded nanoparticles were prepared in same fashion as that of BSA-loaded nanoparticles except the ARH peptide was dissolved in DS solution instead of in the CS solution, with its concentration varied from 0.27 mg mL^{-1} to 0.36 mg mL^{-1}. However, the final

concentration of ARH peptide in the mixture of CS/DS was always kept between 0.18mg mL^{-1} to 0.20 mg mL^{-1}.

2.2.3 Determination of nanoparticle yield

The yield of nanoparticles was determined by decanting the supernatant after the separation of nanoparticles from aqueous suspension medium by centrifugation of solution at 15,000g for 15 min at 4°C and drying the nanoparticles at 60°C to a constant weight. The same volume of water was used as a control. Yield (%) is percent of actual weight of nanoparticles recovered over the sum of total amount of matrix materials (DS and CS) and drug molecule (BSA or ARH peptide) used.

2.2.4 Characterization of CS nanoparticles

Measurements of particle size and zeta potential of the nanoparticles were performed by photon correlation spectroscopy and laser doppler anemometry, respectively, using a Zetasizer 3000HS instrument (Malvern Instrument, UK).

2.2.4.1 Particle size

The particle size measurements were performed using a quartz cell in the automatic mode. The particle size analysis of each sample was performed at 25°C with a detection angle of 90° and ten repeat measurements (22), the raw data were subsequently correlated to Z average mean size by cumulative analysis, performed by the zetasizer 3000 HS software package. Z average mean was defined as average particle size determined by Malvern Zetasizer using photon correlation spectroscopy (PCS). It is known that all particles exhibit Brownian movement, which causes the intensity of light to scatter from

the particles, which then is detected as a change in intensity with time with suitable optics and a photo multiplier. Photon correlation spectroscopy uses the rate of change of light fluctuations to determine the size distribution of the particles scattering light. For convenience, all the particle size (Z average mean) measured by Zetasizer is reported as the mean particle size in our study.

2.2.4.2 Surface properties of nanoparticles

The zeta potential was determined using a Malvern Zetasizer (Malvern Instruments, UK). Measurements were carried out at 25°C with samples diluted in the aqueous solution and injected into the flow cell chamber. All measurements were performed in triplicate with automatic mode.

The performance of the Malvern Zetasizer was checked for its consistence by determining the zeta potential value of a standard solution (DTS0050) supplied by the Malvern Instruments, UK. According to the Malvern, the standard should produce a zeta potential value of 50 ± 5 mV. In our experiment, we calibrated the instrument every time with the standard prior to determining the zeta potential of nanoparticle suspensions.

2.2.4.3 Morphology of nanoparticles

The morphology of the nanoparticles was characterized using a transmission electron microscopy (TEM). Samples for TEM were prepared by dispersing dried nanoparticle powder in distilled water. On the top of the copper grids, a drop of sample solution was placed and allowed to air dry, then coated with carbon. TEM pictures were taken using a CM 12 Philips transmission electron microscope.

2.2.4.4 Evaluation of the protein loading capacities of nanoparticles

The amount of BSA entrapped in the nanoparticles was calculated by the difference between the total amount of protein in the initial formulation medium and the free protein, i.e. amount of non-entrapped protein remaining in the aqueous supernatant. The latter amount was determined following the separation of protein-loaded nanoparticles from the aqueous medium by centrifugation at 15,000 rpm at 4°C for 15minutes. The amount of free protein in the supernatant was determined by the Bradford protein assay method (63). The protein loading (%) of the nanoparticles and the entrapment efficiency (%) were calculated using the equations below. The weight of nanoparticles was obtained in the study of nanoparticle yield.

$$\text{Loading (\%)} = \frac{\text{Total amount of protein - Free protein}}{\text{Weight of nanoparticles}} \times 100 \qquad \text{(Equation 1)}$$

$$\text{Entrapment Efficiency (\%)} = \frac{\text{Total amount of protein - Free protein}}{\text{Total amount of protein}} \times 100 \qquad \text{(Equation 2)}$$

2.2.4.5 Evaluation of ARH peptide encapsulation and loading

Entrapment efficiency and nanoparticle yield for the different formulations containing ARH peptide were determined by the same fashion as described in section 2.2.4.4 with exception that ARH peptide concentrations in supernatant were measured by a fluorescence assay, following fluorescamine derivatization as described in the section 2.2.6 using a fluorescence spectrophotometer, (Cary Eclipse fluorescence spectrophotometer, Varian Technologies) with a slit width of 5nm and excitation and emission wavelengths at 392nm and 485nm, respectively (64). Dilutions of samples and

calibration curves were performed in water, and all measurements were performed in triplicate. Loading capacity and entrapment efficiency were calculated using equation 3 and 4, respectively, after subtracting the blank (supernatant of empty nanoparticles).

$$\text{Loading (\%)} = \frac{\text{Total amount of peptide - Free peptide}}{\text{Weight of nanoparticles}} \times 100 \quad \text{(Equation 3)}$$

$$\text{Entrapment Efficiency (\%)} = \frac{\text{Total amount of peptide - Free peptide}}{\text{Total amount of peptide}} \times 100 \quad \text{(Equation 4)}$$

2.2.4.6 *In-vitro* BSA release from nano-particles

A known quantity of protein loaded nanoparticle suspension was centrifuged at 15,000 rpm for 30 min at 4°C. The details of the centrifuge instrumentation are described in section 2.2.7. The supernatant solution was decanted and the collected nanoparticles were then re-suspended and incubated in 5mL of an aqueous 10mM phosphate buffer pH 7.4 or water with controlled agitation at 37°C. The quantity of nanoparticles was adjusted to obtain a BSA concentration of 1mg mL^{-1} per release study. At designated time intervals samples were centrifuged (15,000 rpm) and 5mL of the supernatant were removed and replaced by an equal volume of the fresh medium (10mM phosphate buffer pH 7.4 or water). The amount of BSA released at various time intervals was determined using the Bradford protein assay method as described in the section 2.2.5. BSA calibration curves were made with fresh BSA dissolved in the incubation medium. All measurements were performed in triplicate.

In all the release study cases the water used had been stocked for less than 2 days, with pH around 5.6-5.8, which, we expect, does not affect the release studies, because in all cases the pH of water is less than the pKa of CS (6.3).

2.2.4.7 *In-vitro* ARH peptide release from nanoparticles

A known quantity of nanoparticles was collected by centrifugation at 12,000 rpm for 30 min at 4°C. The nanoparticles were re-suspended and incubated in 1.45 mL of 10mM phosphate buffer (pH 7.4) or water at 37°C with controlled agitation. The quantity of nanoparticles was adjusted to obtain a final peptide concentration of 0.2mg mL^{-1}(instead of 1mg mL^{-1} as per BSA release study) because of the limited availability of the ARH peptide and its highly sensitive fluorescence assay. At varying time intervals, supernatants were isolated by centrifugation at 12,000 rpm for 30 min at 4°C and measured by the fluorescence assay described in the section 2.2.6. Peptide calibration curves were made with water or 10mM phosphate buffer pH 7.4 and all measurements were performed in triplicate. The centrifugation speed of 12,000 rpm used for peptide release study is different from that of BSA study, in which 15,000 rpm was used. This is due to the high cost of peptide which forced us to use small volumes of peptide-loaded nanoparticle suspension for the release study. Consequently we used a micro-centrifuge (Minispin Eppendorf, Germany), which has a maximum speed of 12,000 rpm, for separation of nanoparticles from the release medium.

2.2.5 Bradford protein assay

The standard Bradford protein macro-assay described in the package insert of Sigma's Bradford reagent was followed. Protein standard solutions with concentrations ranging

from 50μg mL^{-1} to 1000μg mL^{-1} were prepared by dissolving BSA in water or 10mM phosphate buffer pH 7.4. Protein standard solution (100μL) was added into each appropriately labeled tube. 100μL of deionised water was added into a tube labeled blank. The unknown samples were prepared in triplicates with aliquots of 100μL added to each tube. Then to the samples (standard & unknown), 3mL of Bradford reagent was added and the absorbance at 595nm was measured after 2 minutes and before 1hr of the reaction in a 3mL curette against a reagent blank prepared from 0.1mL of the water and 3mL of the Bradford reagent. The absorbance was then plotted against the concentration of protein, which results in a standard curve for determining the protein concentrations in unknown samples.

2.2.6 Fluorescence assay of ARH peptide by the fluorescamine derivatization method

The fluorescamine derivatization method used in this study was adapted from the method described by Bae and his colleagues (5). To each 500μL peptide solution, 500μL of 0.05% w/v fluorescamine dissolved in acetonitrile and 1.5mL of 60mM sodium phosphate buffer pH 9 were added. The solutions were allowed to react at room temperature for 5 min before its fluorescence was measured in a Cary Eclipse fluorescence spectrophotometer (Varian Technologies). Blanks consisting of water, buffer, and fluorescamine in acetonitrile were used to correct for fluorescence background. The amount of peptide in the unknown samples was then quantitated against the corresponding intensity from a standard curve prepared with the known amounts of peptide samples.

2.2.7 Instrumentation of centrifuge

Beckman coulter Allegra 64R centrifuge was used, for separation of nanoparticles from solution, with a F0630 rotor at a speed of 15,000 rpm for 15 min at 4°C with a deceleration rate and acceleration rate of 4 and 6 respectively.

3. Results and Discussion

In the present study we modified the method of Calvo et al. (29) for the formation of a novel nanoparticulate system made of solely hydrophilic polymers. These nanoparticles are composed of cationic and anionic polymers (CS and DS). The manufacturing technique involves the mixture of two aqueous phases (CS and DS) under mild conditions at room temperature. Nanoparticles are formed by coacervation, which is a spontaneous phase separation process arising from electrostatic interactions when oppositely charged macromolecules are mixed together. The success of the process is largely dependent on intermolecular linkages created between the negative groups of DS with that of positively charged amino groups of CS. A similar principle has been used by other research groups for the preparation of nanoparticles (65). The present study, as far as the author is aware, however, is the first attempt reported to use the combination of CS and DS as the matrix materials for incorporation of a protein or a peptide into a nanoparticle system. The advantages of this technique include:

(1) Nanoparticles are prepared under extremely mild conditions and in a short time without involving high temperatures, sonication, or organic solvents.

(2) Particle size and surface charge can be modulated by varying the ratio of CS/DS.

(3) The excellent loading capacity for proteins and peptides and also potentially the continuous release for extended periods of time can be achieved.

All these features make this novel nanoparticulate system a promising carrier for macromolecules, such as peptides, proteins and oligonucleotides.

3.1 Identification of conditions for the formation of CS/DS nanoparticles

For the development of this new nanoparticle system we first conducted a study to identify the experimental conditions at which the CS-DS coacervates could be formed. Experiments were performed by mixing variable volumes and concentrations of DS to 5mL of respective concentrations of CS at room temperature with magnetic stirring. Mixtures, which became turbid, were examined under an optical microscope for evidence of coacervation and analyzed for particle size. A preliminary screening of different CS-DS combinations showed that both polymer ratio and total polymer concentration influenced the formation of coacervates (nanoparticles). Results of this study are represented in Figure 4 and it can be seen that the formation of nanoparticles is possible only for some specific concentrations of CS and DS. The appearance of these preparations was observed microscopically and samples were sized and then classified according to their size as 100–500 nm, 501–1000 nm, and > 1000nm, as shown in Figure 4. It can be seen the smaller particle size was basically confined to very dilute solutions of CS (initial concentration of 0.1% w/v) and DS (initial concentration of 0.1% w/v). The addition of DS to the CS initially resulted in small coacervation nuclei, which coalesced into larger coacervates as the concentrations of the matrix materials increased from 0.25% w/v to 1% w/v. There is one exception where nanoparticles of 370 nm were obtained when 5mL of 0.25% w/v CS was mixed with equal volume of 0.25% w/v DS (Table 3).

It can be noted from the Tables 2, 3, 4 and 5 that the particle size is dependent on both CS and DS concentrations, the higher the final concentration of CS, the larger the particle

size. The minimum size (262 nm) was obtained for the lowest CS and DS concentrations. It is observed that in general, the final concentration of CS has to be controlled below 0.625 mg mL^{-1} with optimum DS final concentration of 0.375 – 0.629 mg mL^{-1} in order to obtain particle size less than 500nm.

From data presented in tables 2, 3, 4, and 5 it was found that the particle size of nanoparticles was dependent on both the concentration and the ratio of the two oppositely charged matrix materials. The particle size of nanoparticles showed a direct correlation to the concentration of CS i.e. as the final concentration of the CS decreases there is a decrease in the particle size, which is consistent with what reported in the literature (29). The smaller size nanoparticles tend to form with the higher ratio of DS in the formulation (Figure 5). This could be attributed to the formation of nanoparticles with higher magnitude of zeta potential by addition of higher ratio of DS which improves the stability of nanoparticle dispersion. We also speculate that the incorporation of DS may have affected the entanglement of the CS chains following the gelation/coacervation process. After assessing the effect of polymer concentrations on the particle size and identifying 0.1% being the optimum polymer concentration, four different CS/DS ratios [5mL:3mL (1.67:1), 5mL:5mL (1:1), 3mL:5mL (0.6:1), and 5mL:8.5mL (0.59:1)] of 0.1% w/v concentrations of CS and DS were investigated further to optimize the formulation of CS/DS nanoparticles for the delivery of proteins and peptides.

Figure 4: Effect of the final concentrations of matrix materials (CS/DS) on the size of nanoparticles formed.

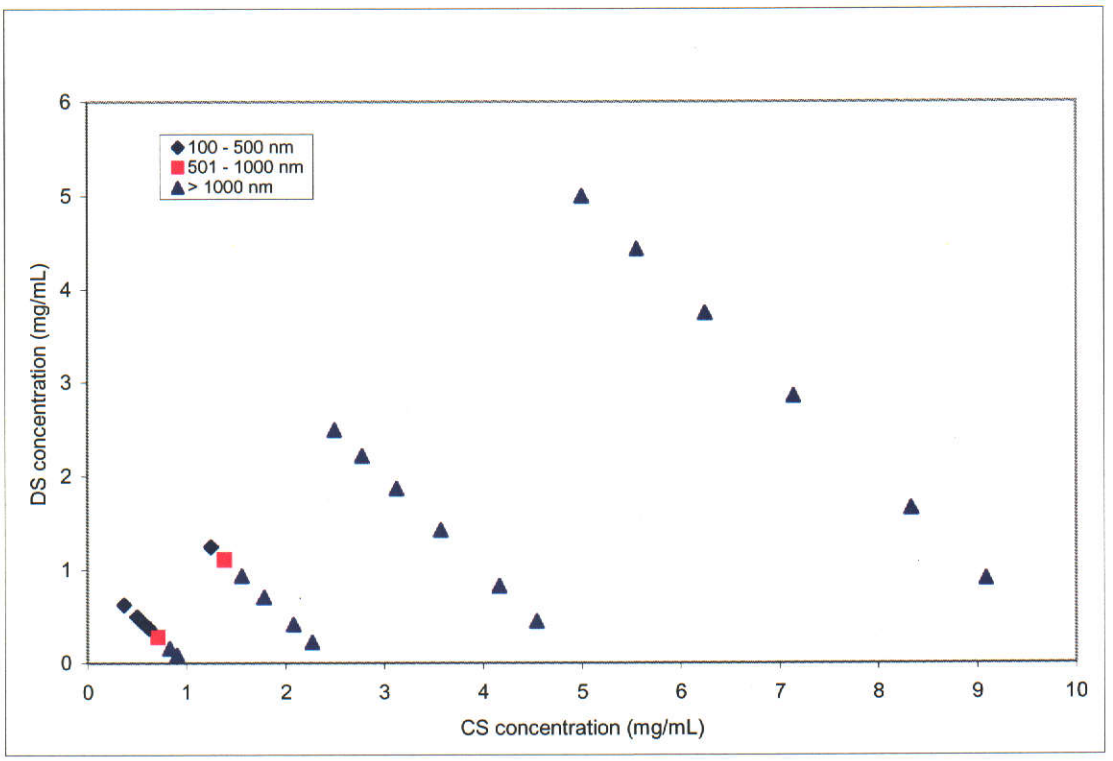

Table 2: Effect of admixture of variable volumes of 0.1% w/v CS and 0.1% w/v DS on the size of nanoparticles formed

CS/DS ratio	Volume of CS added (mL)	Volume of DS added (mL)	Final Concentration of CS (mg/mL)	Final Concentration of DS (mg/mL)	Mean Particle size (nm)
5mL:0.5mL (10:1)	5	0.5	0.909	0.091	1455
5mL:1mL (5:1)	5	1	0.833	0.167	1164
5mL:2mL (2.5:1)	5	2	0.714	0.286	724
5mL:3mL (1.67:1)	5	3	0.625	0.375	494
5mL:4mL (1.25:1)	5	4	0.555	0.444	442
5mL:5mL (1:1)	5	5	0.500	0.500	339
5mL:8.5mL (0.59:1)	5	8.5	0.370	0.629	262

Table 3: Effect of admixture of variable volumes of 0.25% w/v CS to 0.25% w/v DS on the size of nanoparticles formed

CS/DS ratio	Volume of CS added (mL)	Volume of DS added (mL)	Final Concentration of CS (mg/mL)	Final Concentration of DS (mg/mL)	Mean Particle size (nm)
5mL:0.5mL (10:1)	5	0.5	2.272	0.227	8482
5mL:1mL (5:1)	5	1	2.083	0.416	6503
5mL:2mL (2.5:1)	5	2	1.785	0.714	2556
5mL:3mL (1.67:1)	5	3	1.562	0.937	1364
5mL:4mL (1.25:1)	5	4	1.389	1.111	838
5mL:5mL (1:1)	5	5	1.250	1.250	370

Table 4: Effect of admixture of variable volume of 0.5% w/v CS to 0.5% w/v DS on the size of nanoparticles formed

CS/DS ratio	Volume of CS added (mL)	Volume of DS added (mL)	Final Concentration of CS (mg/mL)	Final Concentration of DS (mg/mL)	Mean Particle size (nm)
5mL:0.5mL (10:1)	5	0.5	4.545	0.454	8907
5mL:1mL (5:1)	5	1	4.167	0.833	8061
5mL:2mL (2.5:1)	5	2	3.571	1.429	6011
5mL:3mL (1.67:1)	5	3	3.125	1.875	4490
5mL:4mL (1.25:1)	5	4	2.778	2.222	4462
5mL:5mL (1:1)	5	5	2.500	2.500	3350

Table 5: Effect of admixture of variable volumes of 1% w/v CS to 1% w/v DS on the size of nanoparticles formed

CS/DS ratio	**Volume of CS added (mL)**	**Volume of DS added (mL)**	**Final Concentration of CS (mg/mL)**	**Final Concentration of DS (mg/mL)**	**Mean Particle size (nm)**
5mL:0.5mL (10:1)	5	0.5	9.091	0.909	29676
5mL:1mL (5:1)	5	1	8.333	1.667	37952
5mL:2mL (2.5:1)	5	2	7.142	2.857	35319
5mL:3mL (1.67:1)	5	3	6.250	3.750	23649
5mL:4mL (1.25:1)	5	4	5.555	4.445	23013
5mL:5mL (1:1)	5	5	5.000	5.000	9591

3.2 Characterization of BSA-loaded CS/DS nanoparticles

3.2.1 Particle size and zeta potential

Due to the high cost of ARH peptide, BSA was used initially as a model protein in this study. BSA-loaded nanoparticles were obtained spontaneously upon addition of variable volumes (1mL, 3mL, 5mL and 8.5mL) of the DS aqueous solution (0.1%w/v) to 5mL of the CS solution (0.1% w/v) with magnetic stirring. The incorporation of BSA in the CS/DS nanoparticles was achieved by dissolving the protein either in the CS solution before mixing with DS or in the DS solution prior to mixing with CS solution. The influence of the matrix materials ratio on the physico-chemical characteristics of empty and BSA-loaded nanoparticles is presented in Table 6. It is seen that nanoparticles of varying characteristics can be obtained with different ratios of CS and DS. The size and zeta potential of these nanoparticles can be conveniently modulated by varying the ratio of CS to DS.

For each particle size determination, Malvern's Zetasizer produces particle size histogram (intensity) and automatically converts it to calculate the Z average mean size in nm. A typical histogram is presented in the Appendix 3.

The positively charged CS has the ability to interact electrostatically with negatively charged macromolecules, in this case, DS. The CS molecules are ionically cross-linked with DS, via the electrostatic interaction between the sulfate groups of DS and amino groups of CS to form solid nanoparticles. As the isoelectric point of BSA is 4.8, at any pH below 4.8 BSA would be positively charged. In our case the pH of the nanoparticles

formulation medium (3.55-4.05) is below BSA's isoelectric point, hence BSA should be positively charged and could compete with CS to interact with DS electrostatically. This ionic interaction, provided by the multi-ionic sites of the large molecule BSA might have contributed to the strong association of BSA with the nanoparticles, which is reflected by the high level of incorporation and slow release of BSA (see the later sections). Other mechanisms such as hydrophobic interactions, hydrogen bonding, and even physical entrapment may also be responsible for the association of BSA with the nanoparticles.

One interesting feature from Table 6 (Figure 5 & 6) is the decrease in particle size and change of surface charge from positive to negative as the volume of dextran sulfate was increased from 3mL (CS/DS ratio:1.67:1) to 8.5mL (CS/DS:0.59:1). This feature can be very advantageous in achieving high level loading of positive charged proteins or peptides, also suggesting that ionic interaction could play a major role for the incorporation of protein and peptide. The change of zeta potential in both sign and magnitude, when comparing empty to the BSA loaded nanoparticles prepared from CS/DS ratio of 5mL:5mL (1:1) to 5mL:8.5mL (0.5:1), clearly supports the hypotheses that BSA association with nanoparticles can be modulated by its ionic interaction with oppositely charged ionic polymer (DS in our case) in the nanoparticles. The nanoparticles produced from CS/DS ratios 3mL:5mL (0.6:1) and 5mL:8.5mL (0.59:1), seen in Table 6, are very similar. Initially we started with 3mL:5mL (0.6:1) ratio to study its effect on physico-chemical characteristics of BSA loaded nanoparticles. In order to keep the volume of CS constant in all cases, we later adopted 5mL:8.5mL (0.59:1) ratio. It can be seen that the results obtained from both were more or less the same (Table 6).

It is noted that there is a reduction in zeta –potential of BSA-loaded nanoparticles in comparison to that of empty nanoparticles when the CS/DS ratio is 5mL:3mL (1.67:1). This could be due to that fact that BSA is a macromolecule with many functional groups and it is possible that it forms other types of binding with matrix materials. This may be significant when the concentration of DS is relatively low, thus changing the distribution of negatively charged groups on the surface of nanoparticles. Another reason for this against trend data could be due to a large error in the determination of zeta-potential of the sample with this particular ratio because much larger particles were formed.

The increase in particle size, with corresponding reduction of zeta potential (Table 6) of these BSA-loaded nanoparticles, compared to the empty ones, is also a good indication of the incorporation of BSA in the nanoparticle's structure. It is interesting to see an increase in the final concentration of DS leads to the reduction of the size and the positive charge of the nanoparticles. The empty nanoparticles prepared from the CS/DS ratio 5mL:1mL (5:1) to 5mL:8.5mL (0.59:1) showed a change in surface charge from positive to negative as the volume of DS was increased. This change in charge is attributed to the presence of negatively charged DS at the particle surface as there are more sulfate groups than amino groups in the formulation, when CS/DS ratio increases to 5mL:5mL (1:1) or 5mL:8.5mL (0.59:1) based on molar ratio calculation of the CS and DS molecules. On the other hand, the increase in size was observed when BSA was incorporated suggests that BSA might have formed close association with nanoparticle matrix material. BSA-loaded nanoparticles had a greater reduction in zeta potential than corresponding empty

nanoparticles as the CS/DS ratio increases from 5mL:5mL (1:1) to 5mL:8.5mL (0.59:1) (Table 6). This difference could be due to the various binding / association mechanisms BSA involved with nanoparticles at different CS/DS ratio.

As mentioned previously, we expect BSA to ionically interact with CS and DS differently, under our experimental conditions. To assess the order of BSA mixing, characteristics and entrapment efficiency of nanoparticles, we compared BSA-loaded nanoparticles prepared by either dissolving the BSA in CS or in DS. No significant difference was found in most of their physico-chemical characteristics of the CS/DS nanoparticles with exception of zeta potential (Table 7).

Table 6: Influence of the ratio of matrix materials (CS/DS) on the physico-chemical characteristics of empty and BSA loaded nanoparticles, prepared using 0.1% w/v CS and 0.1% w/v DS.

Sample	CS/DS ratio	pH of preparation	Mean Particle Size (nm)*	Zeta Potential (mV)
Empty	5mL:1mL (5:1)	3.55	1270 ± 150	72.9
Empty	5mL:3mL (1.67:1)	3.75	494 ± 40	52.7
Loaded	5mL:3mL (1.67:1)	3.87	1138 ± 100	26.4
Empty	5mL:5mL (1:1)	3.65	435 ± 40	-23.7
Loaded	5mL:5mL (1:1)	3.93	891 ± 115	30.0
Empty	3mL:5mL (0.6:1)	3.99	350 ± 50	-32.3
Loaded	3mL:5mL (0.6:1)	4.04	478 ± 45	-28.0
Empty	5mL:8.5mL (0.59:1)	3.67	293 ± 5	-32.9
Loaded	5mL:8.5mL (0.59:1)	3.72	660 ± 24	-26.6

*Size measurement data are the average value of four measurements ± one standard deviation. (n=4)

Table 7: Comparing the influence of BSA incorporation into the matrix materials on the physico-chemical characteristics of 5mL:8.5mL (0.59:1) CS/DS nanoparticles.

Sample	CS/DS ratio	Mean Particle Size (nm)	Zeta Potential (mV)	Loading (%)	Entrapment efficiency (%)	Yield (%)
BSA dissolved in CS	5mL:8.5mL (0.59:1)	660 ± 24	-26.6	24.1	100.0	92.7
BSA dissolved in DS	5mL:8.5mL (0.59:1)	610 ± 18	-15.4	30.8	100.0	92.0

Figure 5: Particle size and Zeta Potential of empty nanoparticles.

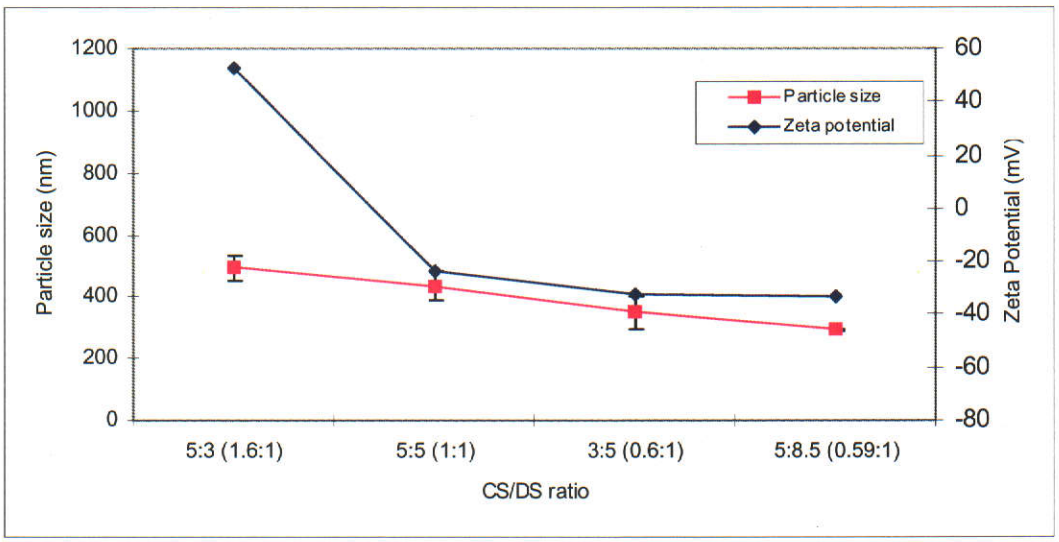

Figure 6: Particle size and Zeta Potential of BSA loaded nanoparticles.

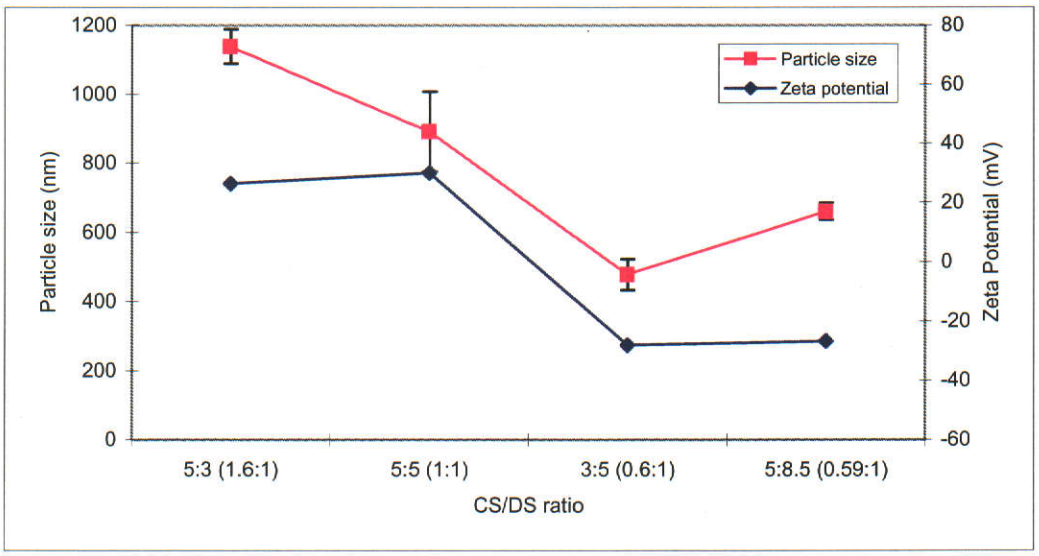

3.2.2 Morphology of empty and BSA-loaded CS/DS nanoparticles

Transmission electron microscopy (TEM) images of empty and BSA-loaded CS/DS nanoparticles prepared from the 5mL:8.5mL (0.59:1) ratio are shown in the figure 7, 8, 9 and 10. It is seen that these particles have a solid and near consistent structure. Furthermore, the incorporation of BSA into the nanoparticles by dissolving in either CS or DS solution produced nanoparticle with a more smooth surface and compact structure. The particle size observed in TEM is in consistent with that measured by the Zetasizer.

Figure 7: Transmission electron micrograph of empty CS/DS nanoparticles (CS/DS 5mL:8.5mL).

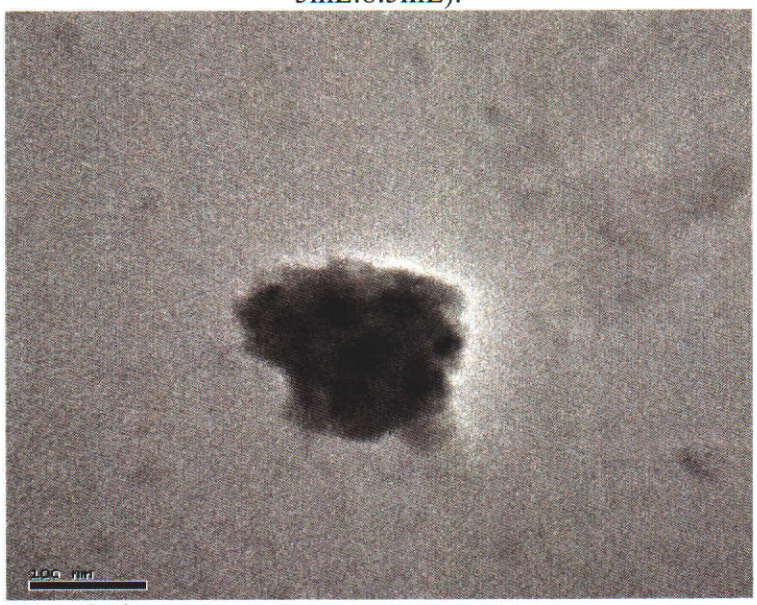

100nm Scale

Figure 8: Transmission electron micrograph of empty CS/DS nanoparticles (CS/DS 5mL:8.5mL).

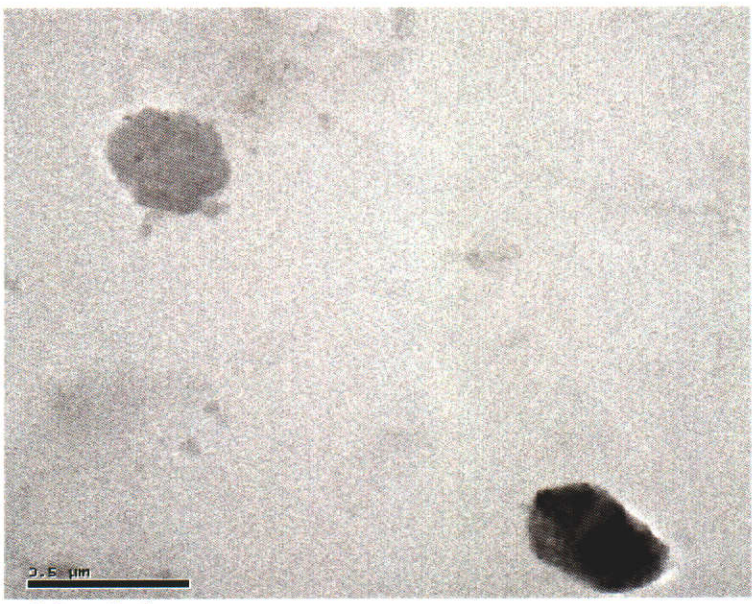

0.5µm Scale

Figure 9: Transmission electron micrograph of BSA loaded CS/DS nanoparticles [(CS/DS 5mL:8.5mL) BSA dissolved in DS solution].

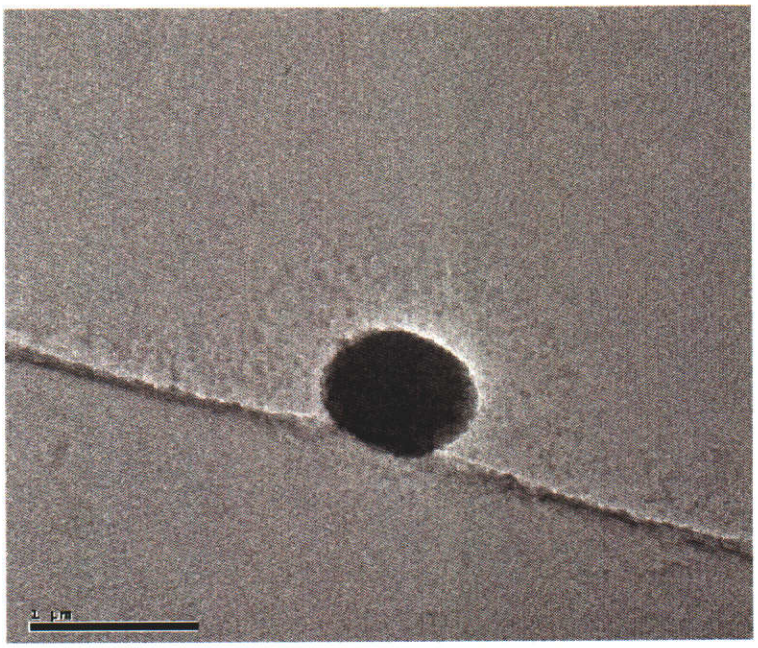

1µm Scale

Figure 10: Transmission electron micrograph of BSA loaded CS/DS nanoparticles [(CS/DS 5mL:8.5mL) BSA dissolved in CS solution].

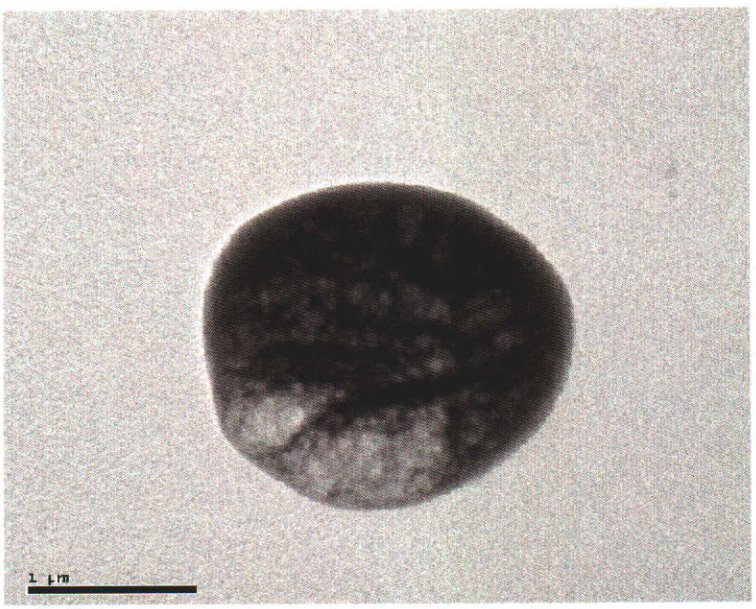

1µm Scale

3.2.3 BSA Loading and entrapment efficiency

Results of the entrapment efficiency and protein loading capacity of the four different ratios of nanoparticles are displayed in Table 8 and in Figure 11. It was seen that the BSA entrapment efficiency was affected by the ratio of DS, the higher the DS ratio the higher the entrapment efficiency. The maximum entrapment efficiency 100% was achieved with CS/DS ratio of 5mL:8.5mL (0.59:1). However, the protein loading capacity reached maximum when CS/DS ratio was 5mL:5mL (1:1) with 33.7 mg of BSA entrapped in 100mg of nanoparticles. This loading is best when compared to our calculation of theoretical loading (i.e. the highest loading efficiency). Comparing to results reported by Calvo et al. (28) (BSA entrapment efficiency of 25.8%, 26.8% and 39.1% at pH 3, 4 and 5 respectively with BSA initial concentration of 1mg mL^{-1}, dissolved in CS), we obtained a much higher entrapment efficiency (53.2-100%) at the equivalent pH conditions (Table 8). It is worth pointing out that entrapment efficiency was determined directly whereas the loading value was calculated based on the nanoparticle yield and entrapment efficiency.

Protein association studies carried out by the Calvo's group at different pH values (28) indicated that there was significant BSA entrapment at all pH values but the greatest loading efficiency was obtained when the protein was dissolved at a pH above its isoelectric point, (i.e. when BSA was predominantly negatively charged). This suggests the major factor that lead to the association of protein to the nanoparticle might be the protein-polysaccharide electrostatic interaction as well as other forces including hydrogen bonding, hydrophobic interactions and the reduction of the solubility of BSA near its

isoelectric point. In our case, BSA was positively charged when it was dissolved in CS solution (pH 3.57-3.63), therefore capable of establishing ionic interaction with negatively charged DS during the formulation process. The fact that the entrapment efficiency increased with the DS ratio and the magnitude of negative charge of nanoparticles strongly supports that ionic interaction is the major factor contributing to the entrapment of BSA in our studies with nanoparticles prepared by dissolving BSA in CS.

In our study a cloudy preparation was obtained when BSA (concentration 1mg mL^{-1}) was incorporated into a DS solution (pH 4.6-4.8). Taking into account that the isoelectric point of BSA is 4.8, and at pH near 4.8, the BSA is expected to have minimum charge and therefore the lowest solubility, which might have resulted in a cloudy preparation when it was mixed with DS suspension. It is possible, in this case, that in addition to electrostatic interaction, other mechanisms such as hydrophobic interactions, hydrogen bonding, and other physicochemical forces including physical entrapment could also be responsible for the entrapment and association of BSA with nanoparticles. A significant amount of BSA (at least 10% loaded BSA) could be associated to nanoparticles via mechanisms other than ionic interactions as revealed by the release study of BSA in deionised water described in the section 3.5.

Table 8: Influence of the ratio of matrix materials (CS/DS) on the drug loading and entrapment efficiency of BSA loaded nanoparticles.

CS/DS ratio	Loading (%)		Entrapment efficiency (%)	pH of CS solution	pH of DS solution	Yield (%)
	Theoretical	Actual				
5mL:3mL (1.67:1)	38.5	29.3 (76.1%)*	53.2	3.63	4.87	94.3
5mL:5mL (1:1)	33.3	33.7 (101.2%)*	98.9	3.63	4.79	62.2
3mL:5mL (0.6:1)	27.3	22.7 (83.2%)*	96.8	3.57	4.76	94.9
5mL:8.5mL (0.59:1)	27.0	24.1 (89.3%)*	100.0	3.59	4.79	92.7

* Values in bracket are percent of actual loading over theoretical loading (i.e. Loading efficiency). Theoretical loading values represent the maximum loading a system can achieve; based on the initial amount of BSA incorporated to polymer matrix materials.

Figure 11: Effect of ratio of matrix materials (CS/DS) on BSA loading and entrapment efficiency.

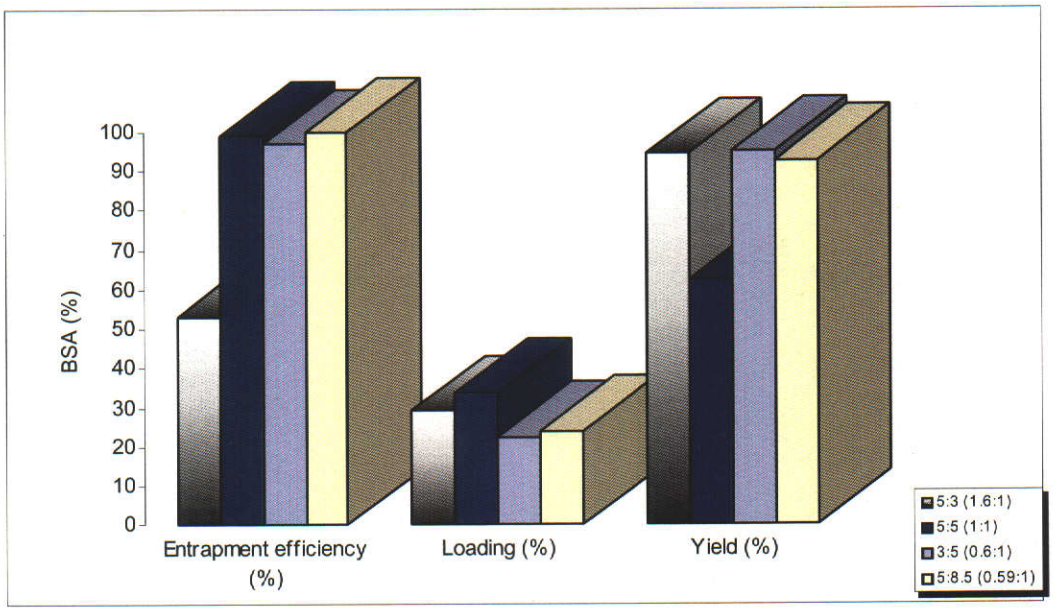

Figure 12: Linear absorbance profile exhibited by BSA standards measured by Bradford protein assay method.

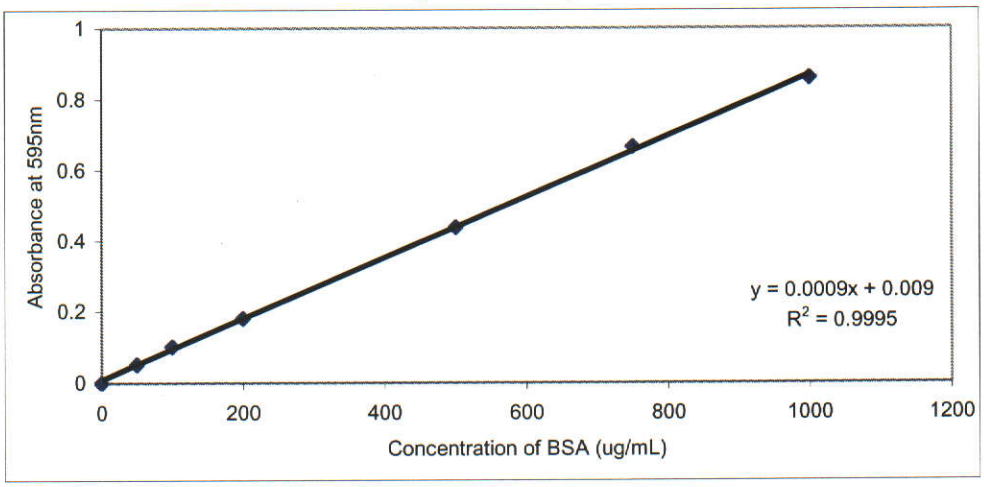

The amount of BSA incorporated into nanoparticles was analyzed using the Bradford protein assay method. It is one of several simple methods commonly used to determine the total protein concentration of a sample. The method is based on the proportional binding of the dye Coomassie blue to proteins. The protein concentration of a test sample is determined by comparison to that of a series of protein standards known to reproducibly exhibit a linear absorbance profile. A typical protein standard curve obtained in our assay is shown in the Figure 12.

The consideration for the use of Bradford assay is based on its fast reaction with reproducible linear response (R^2 >0.999). The technique involves only one mixing step, no heating required, and produces a stable colorimetric response (68).

Unlike many other assays, the Bradford assay is not susceptible to interference by a wide variety of chemicals present in samples. The notable exception is high concentrations of detergents. The Bradford protein assay is well established for BSA analysis (66). It allows the detection of BSA concentrations as low as 1μg mL^{-1}. It is frequently employed by researchers to determine BSA concentration in nanoparticles or microsphere formulations (67). In our study we found that the interference of the Bradford protein assay is related to the concentration of free chitosan (Appendix 1). By subtracting the absorbance measured in the empty nanoparticles (control), we were able to calculate the minimum BSA loading in the worst scenario case, i.e. with maximum free BSA in the system.

3.2.4 *In Vitro* release of BSA from CS/DS nanoparticles

Albumin nanoparticle formulations, prepared under the experimental conditions were tested for *in vitro* release at 37°C. Figure 13, 14, 15, 16, 17, 18, 19 and 20 shows the plot of the data expressed as cumulative percentage as well as differential release of BSA *in vitro* from nanoparticles prepared with various ratios of CS/DS, as a function of time. All data shown are the mean ± standard deviation (n=3). BSA-loaded nanoparticles presented in Figure 13-20, were prepared by dissolving BSA in CS solution, whereas, Figure 21 and 22, were by dissolving BSA in DS solution.

It can be seen from the results obtained with these novel CS/DS nanoparticles, that the release rate is highly affected by the nature of the interactive forces between the associated BSA macromolecule and the matrix material as well as by the ionic nature of the release medium. The interesting observation was that a consistent low portion of BSA (less than 13% loaded BSA) was released in water over the 7 day period. The majority release occurred in the first two time points (12 and 24hrs) irrespective of the ratio of CS/DS (Figure 19 & 20). In comparison, the same batch of nanoparticles, when exposed to 10mM phosphate buffer pH 7.4, showed continuous release of BSA over 7 days (Figure 17 & 18). There was an initial small burst release, corresponding to the level of release of BSA in water, suggesting that the burst release may arise from the desorption of those loosely attached BSA from the surface of the matrix polymers. Though dissociation appears to be the principle mechanism, other factors, such as diffusion of physically entrapped BSA, may also have a role in the release process.

It is noted, when 10mM phosphate buffer pH 7.4, was used as a release medium, that BSA released at a relatively continuous rate for 5:5 (1:1) and 5:8.5 (0.59:1) ratios of CS/DS nanoparticles. It is seen that 31% and 40% of BSA were released in 7 days for 5mL:8.5mL (0.59:1) and 5mL:5mL (1:1) ratio of CS/DS nanoparticles, respectively (Figure 17 & 18). It appears that 5mL:5mL (1:1) ratio nanoparticles released BSA faster than that of the 5mL:8.5mL (0.59:1) system. It depicts the higher the concentration of DS in the nanoparticles preparation medium, the slower was the release of BSA from the nanoparticles. The dissociation of BSA from nanoparticles via ionic-exchange appears to govern the release process in the second phase i.e. from day 2 onward.

The small size of the nanoparticles is also a major factor, which influences the release rate. These nanoparticles have a large surface area due to their small size; therefore a significant portion of the BSA will be at or near the particle surface and can be readily released. Furthermore, the diffusion distances encountered in the particles are small which allows the release medium and the ions to diffuse in readily to exchange with BSA. However, due to the large molecular size of BSA, it is expected to diffuse out slowly even when it becomes dissociated.

It is noted that the *in vitro* release rate behavior of BSA-loaded CS/DS nanoparticles was affected by their level of loading. Calvo et al. (28, 29) observed the percentage *in vitro* release of BSA from CS/DS nanoparticles was greater for those formulations containing a higher protein loading; our finding is consistent with their observation. In our study the

BSA loading capacity of 5mL:8.5mL (0.59:1) ratio CS/DS nanoparticles is 24.1% w/w compared to that of 5mL:5mL (1:1) which is 33.7% w/w, and the release rate of 5mL:5mL (1:1) ratio of CS/DS nanoparticles is faster than that of 5mL:8.5mL (0.59:1) ratio in 10mM phosphate buffer pH 7.4. This might also be attributed to the higher proportion of DS in nanoparticles, in other words, a larger proportion of positively charged BSA might be bound to the negative DS in 5mL:8.5mL CS/DS nanoparticles via ionic interaction, therefore, released slowly. Overall these results suggest that the level of BSA released from nanoparticles can be modulated, simply by adjusting the composition of the CS/DS in nanoparticles or the protein loading.

It was also observed that the different order of incorporation of BSA into nanoparticle formulation medium (i.e. dissolving in CS solution or in DS solution) prior to the formation of nanoparticles seems to have some but not a significant effect on the release behavior of nanoparticles. Figure 21 and 22 depicts the release profiles of nanoparticles prepared from BSA dissolved in DS. The system prepared from BSA dissolved in DS appeared to release more BSA in the buffer, but less in water than that of BSA dissolved in CS (Figure 15, 16, 21 and 22). This marginally higher release of the former over 7 days might be due to weak ionic-interactions with the nanoparticulate matrix caused by the reduced charge of BSA in the DS solution. In fact the relatively low level of BSA release in water may correspond to the larger BSA fraction entrapped in the polymer matrix, instead of adsorbed onto the carrier surface, due to the reduced solubility of BSA at isoelectric point in DS solution.

Figure 13: Cumulative release of BSA from nanoparticles prepared by mixing 5mL of 0.1% w/v CS with 5mL of 0.1% w/v DS, CS/DS ratio 5mL:5mL (1:1); Loading 33.7% w/w.

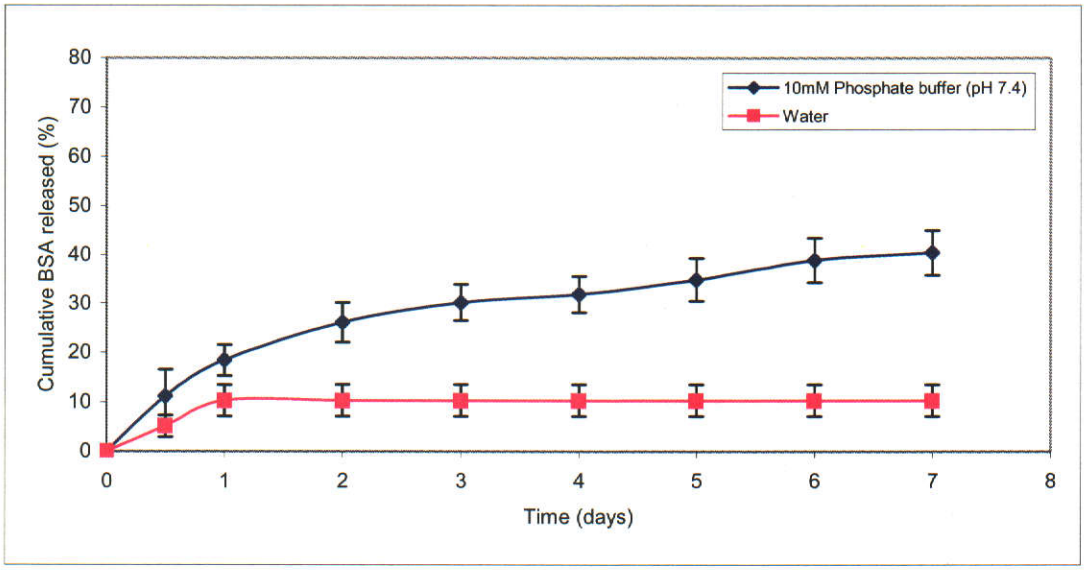

Figure 14: Differential release of BSA from nanoparticles prepared by mixing 5mL of 0.1% w/v CS with 5mL of 0.1% w/v DS, CS/DS ratio 5mL:5mL (1:1); Loading 33.7% w/w.

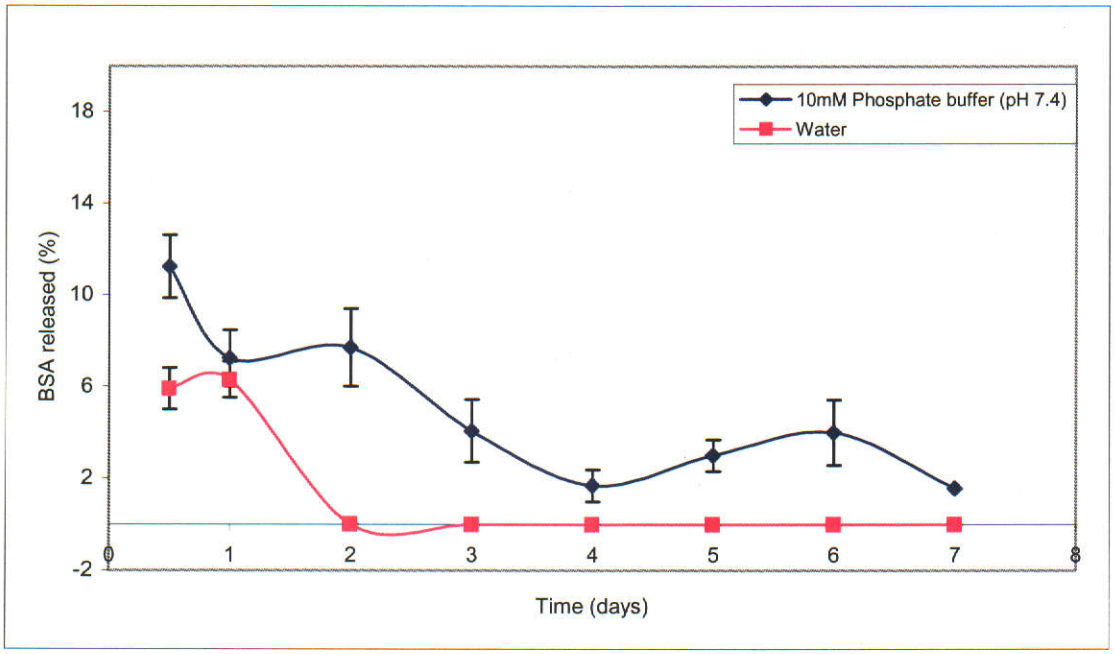

Figure 15: Cumulative release of BSA from nanoparticles prepared by mixing 5mL of 0.1% w/v CS with 8.5mL of 0.1% w/v DS, CS/DS ratio 5mL:8.5mL (0.59:1); Loading 24.1% w/w.

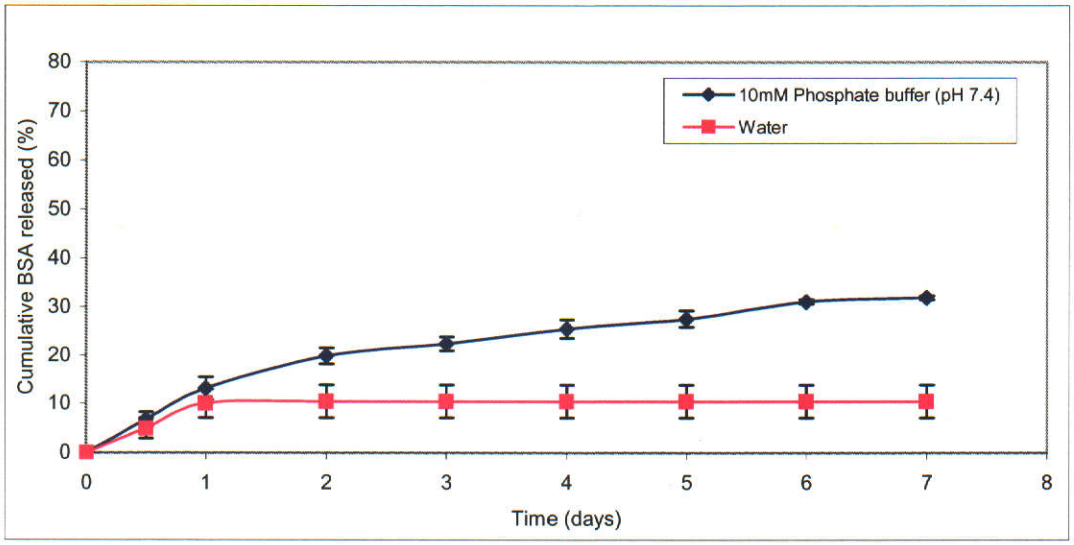

Figure 16: Differential release of BSA from nanoparticles prepared by mixing 5mL of 0.1% w/v CS with 8.5mL of 0.1% w/v DS, CS/DS ratio 5mL:8.5mL (0.59:1); Loading 24.1% w/w.

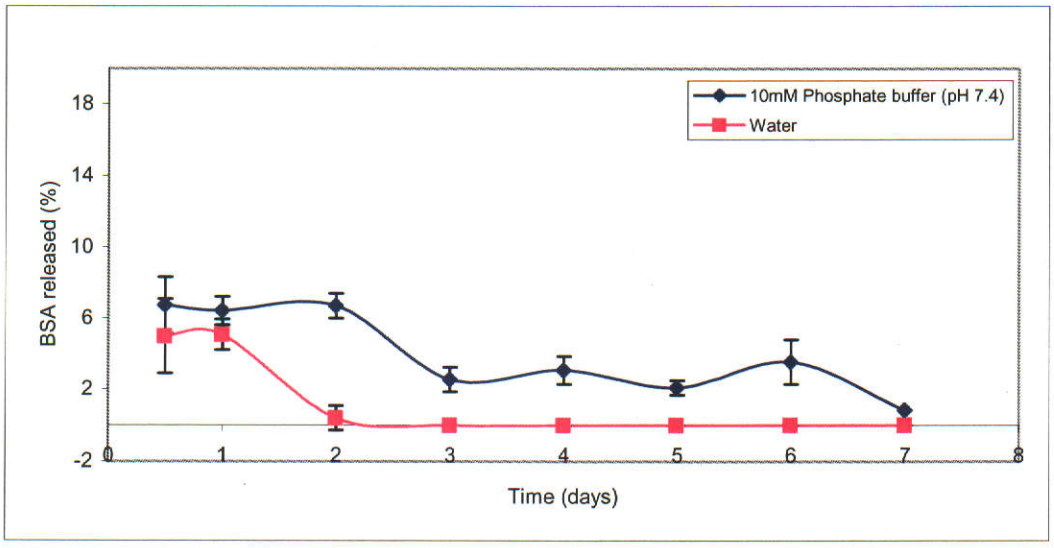

Figure 17: Cumulative release of BSA loaded CS/DS nanoparticles in 10mM phosphate buffer (pH 7.4).

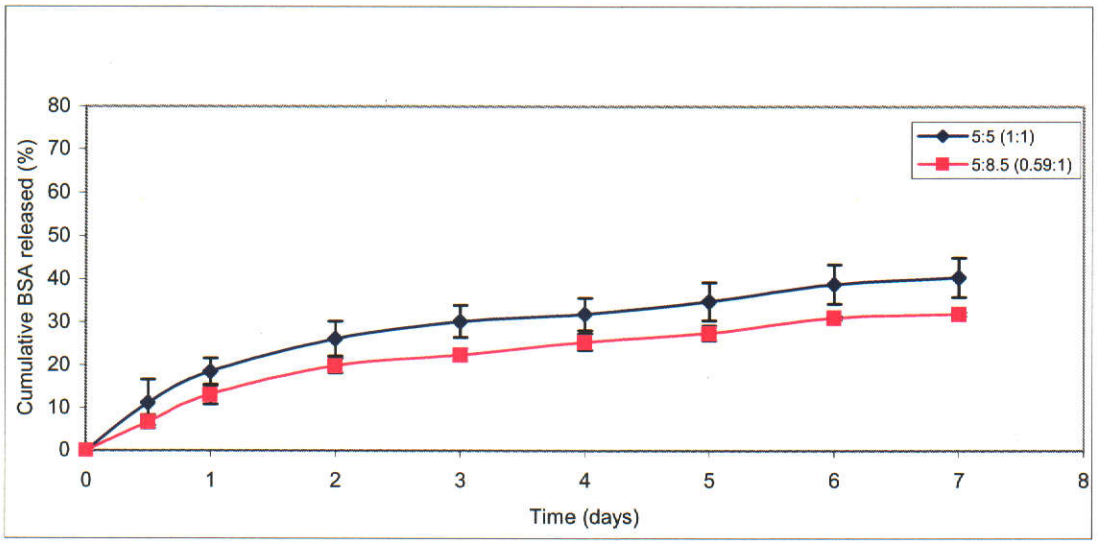

Figure 18: Differential release of BSA loaded CS/DS nanoparticles in 10mM phosphate buffer (pH 7.4).

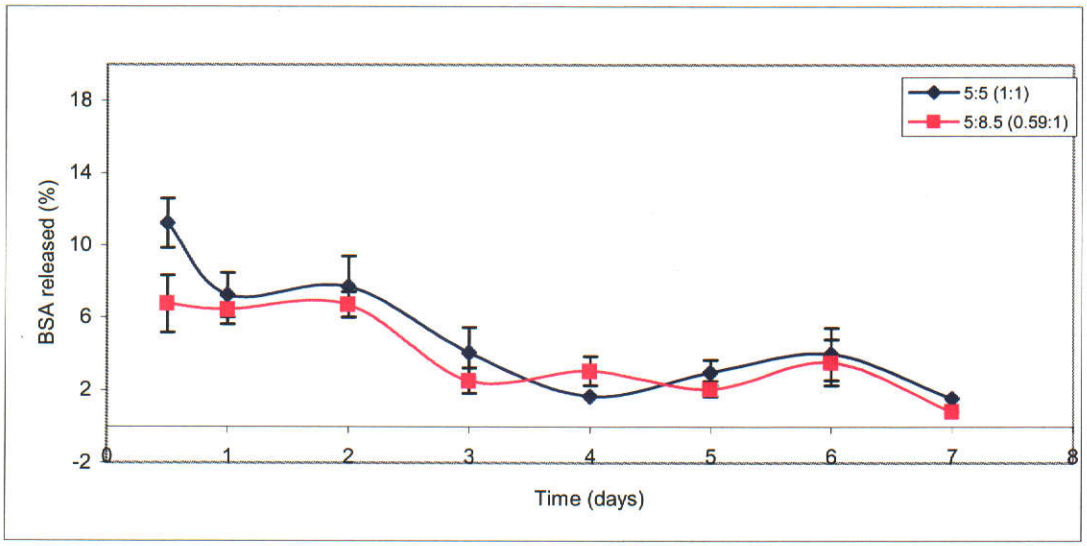

Figure 19: Cumulative release of BSA loaded CS/DS nanoparticles in water.

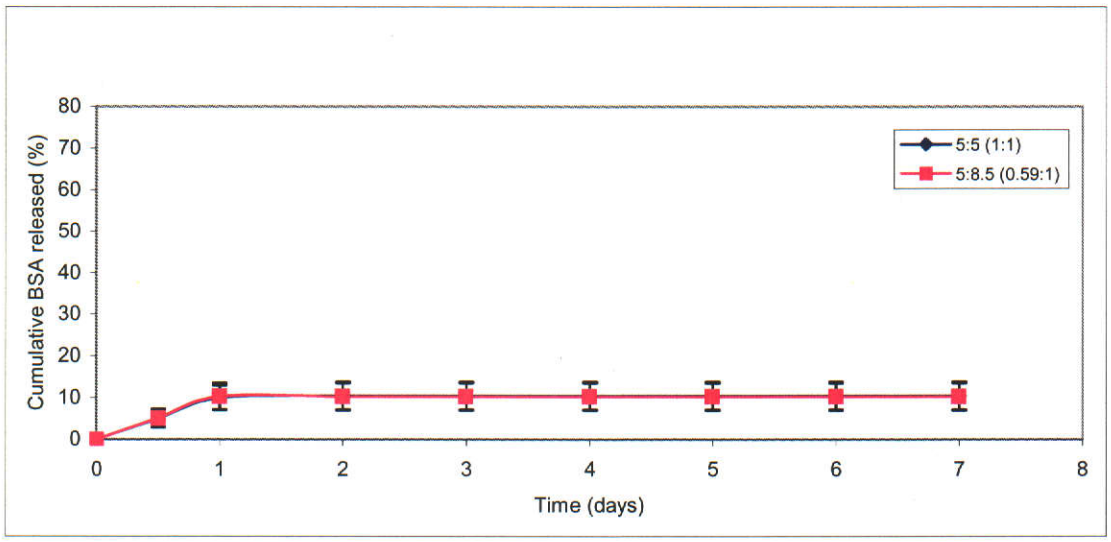

Figure 20: Differential release of BSA loaded CS/DS nanoparticles in water.

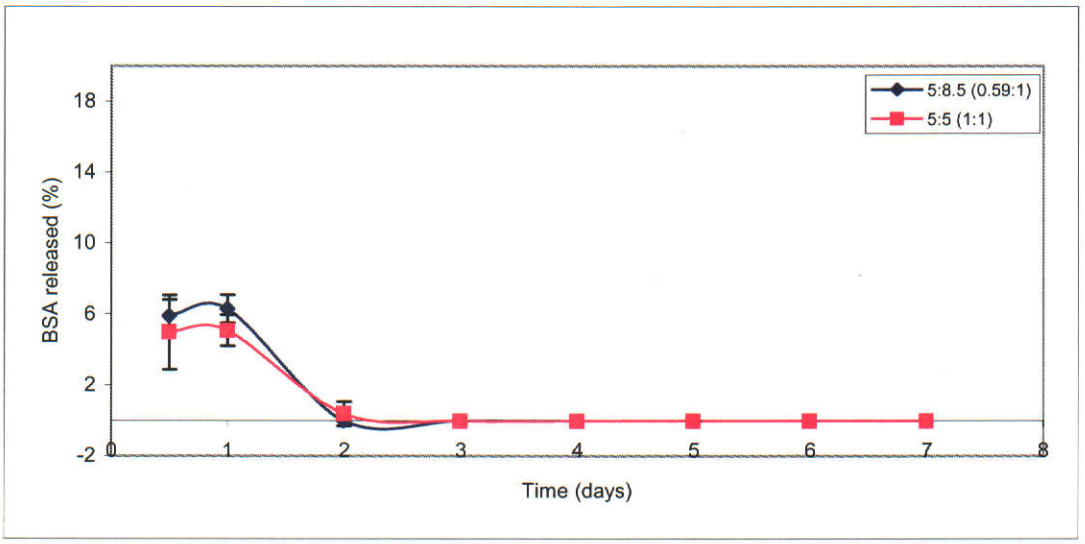

Figure 21: Cumulative rate of release of BSA (dissolved in DS) from nanoparticles prepared by mixing 5mL of 0.1% w/v CS with 8.5mL of 0.1% w/v DS, CS/DS ratio 5mL:8.5mL (0.59:1); Loading 30.8% w/w.

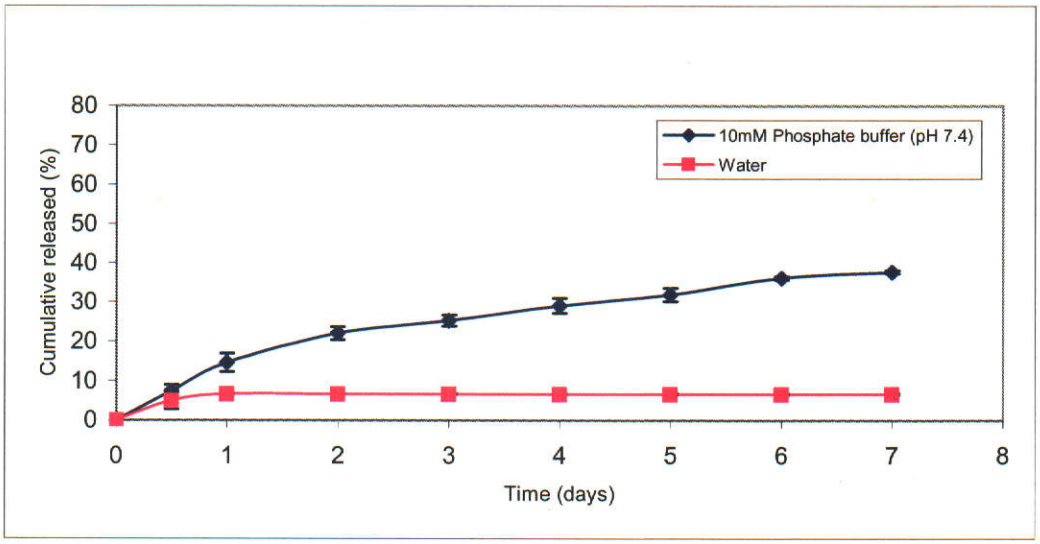

Figure 22: Differential release of BSA (dissolved in DS) from nanoparticles prepared by mixing 5mL of 0.1% w/v CS with 8.5mL of 0.1% w/v DS, CS/DS ratio 5mL:8.5mL (0.59:1); Loading 30.8% w/w.

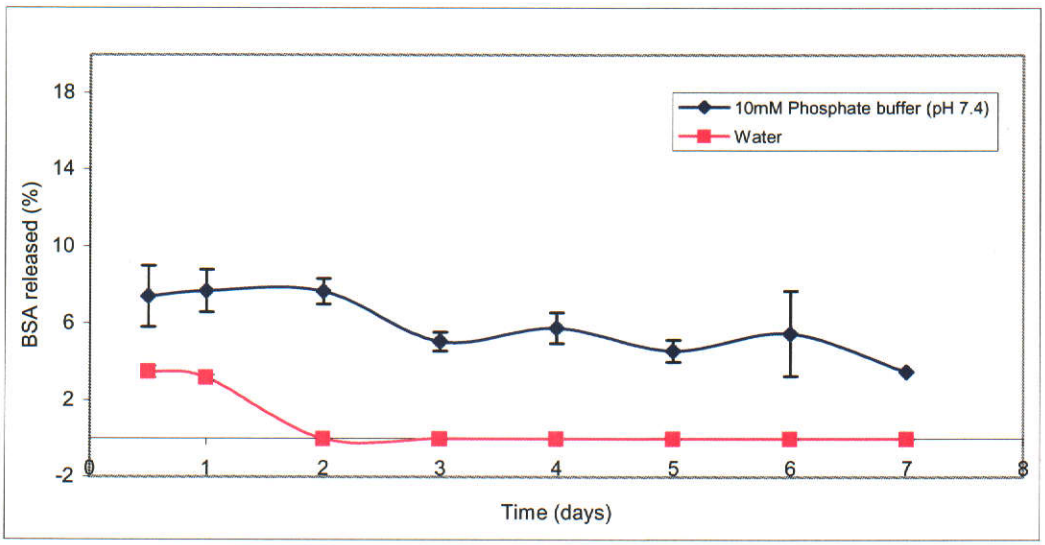

From our studies with BSA, we can conclude that these CS/DS nanoparticles can offer some attractive features which favour them as a promising carrier for the further study of peptide delivery. These features include:

1. Formation of nanoparticles can be achieved under extremely mild conditions.
2. Particle size and surface charge that can be conveniently modulated.
3. Levels of loading and entrapment efficiency can be enhanced by increasing the ratio of oppositely charged polymers, suggesting ionic interaction can be utilized for the high level of protein and peptide incorporation.
4. Sustained release over a week period in the buffer but not in water, suggests the majority of protein was released via ion exchange mechanism.

The major goal of this work was to develop a CS/DS nanopaticulate system as a novel carrier for the ARH peptide. The BSA study revealed the significance of ratio of positively charged CS to negatively charged DS on the formation and sustained release from nanoparticles. In the second part of the study, we applied the same principle to the design of CS/DS nanoparticulate formulations for the positively charged ARH peptide.

3.3 Development of a nanoparticle formulation for ARH peptide incorporation

The electrostatic interactions between anions and CS has an important influence on the properties of the ionically cross-linked CS nanoparticles. Though CS and DS matrices have been used in the pharmaceutical industry for many years, to our knowledge little information concerning the interaction between DS and CS has been reported. Sufficient charge numbers are necessary for anions to cross-link CS by electrostatic force. DS is a polyvalent anion and carries 65 negative charges per mole, equivalent to 6.5×10^{-3}

deprotonated sulfate groups per gram DS under the experimental condition. On the other hand, CS used in our experiment is a weak poly base with 2259 positive charges per mole, equivalent to approximately 5.6 x 10^{-3} protonated amine groups per gram CS under the experimental condition. This is because the net charge number of the DS and CS are mainly controlled by the solution pH (30). CS, at a low solution pH (especially less than pK_a of CS 6.3), has a high degree of ionization of the amine groups. In our study, pH of CS solution (3-4) is well below its pKa, hence, degree of ionization of amino groups of CS is expected to be greater than 99%, whereas, DS'sulfate group is negatively charged, thereby resulting in ionic interaction between CS and DS.

For incorporation of ARH peptide into nanoparticles, we selected three different ratios of CS/DS to formulate nanoparticles; 5mL:5mL (1:1), 5mL:8.5mL (0.59:1) and 5mL:10mL (0.5:1). This selection is based on our observation that when the ratio of CS/DS is 5mL:5mL (1:1) or above (i.e. even higher proportion of DS) in the formulation, the surface charge of the empty nanoparticles is negative, which is consistent with our prediction based on the calculation of charge ratio between the two. Since the ARH peptide is positively charged, we chose these three ratios, with an aim to achieve a strong ionic interaction between the peptide and CS/DS nanoparticles, which in turn might encapsulate appreciable quantities of ARH peptide.

The amounts of non-entrapped ARH peptide and the peptide release samples were determined by a fluorescence assay method. This determination of ARH peptide in the supernatants as well as release samples was rapid and reproducible. The assay is based on

detection of fluorescence produced by the reaction of fluorescamine with amino acids released upon hydrolysis of the peptide amide bond. This method is well established for determination of total concentrations of amino acids in biological samples such as extracts from marine organisms and plants and the cerebrospinal fluid of patients with meningitis (69). Amino acids react with fluorescamine to produce a final product with stable fluorescence to allow their total concentrations determined by fluorimetric measurement. This method was found to be accurate and sensitive, producing linearity over the peptide concentration (from 0.4μg mL^{-1} to 40μg mL^{-1}) with a co-efficient correlation value (R^2) close to 0.9994. Figure 23 shows a typical fluorescence intensity plot as a function of increasing amounts of ARH peptide.

3.3.1 Preparation of ARH peptide-loaded CS/DS nanoparticles

ARH peptide-loaded CS/DS nanoparticles were prepared by the same protocol as described for the BSA study. In all cases, however, the peptide was dissolved in the DS solution. This is because dissolving the peptide in CS solution may produce a repulsion between CS and the peptide, owing to their positive charges. From our BSA study, it is noted that dissolving BSA in either of the polymer solutions, does not have a great impact on the results. However, it was envisaged that electrostatic interactions between the amino groups of the peptide and the sulfate groups of DS might facilitate the association of peptide to the CS/DS nanoparticles. Table 9 compares the size and surface charge of peptide-loaded CS/DS nanoparticles prepared from different CS/DS ratios.

3.4 Characterization of ARH peptide-loaded CS/DS nanoparticles

3.4.1 Particle size and zeta potential

Similar to the findings in the BSA study, incorporation of peptide into nanoparticles also resulted in augmentation of both size and zeta potential of nanoparticles (Table 9 and Figures 24 and 25).

The increase in particle size and change in the magnitude of zeta potential (Table 9) of these nanoparticles is a good indication of the incorporation of peptide in the nanoparticle's structure. These results are in consistent with the BSA study. As stated earlier, it is not surprising that an increase in concentration of DS led to the reduction of the size of the nanoparticles. The increase in the magnitude of zeta potential leads to more stable colloidal dispersion. Results presented in Table 9 indicate that the particle size is, as previously reported (29), dependent upon the CS concentration, the minimum size of nanoparticles corresponding to the lowest CS concentration. This could be due to the reduction of viscosity of CS solution after addition of DS. The CS/DS empty nanoparticles with CS/DS ratio 5mL:5mL (1:1) to 5mL:10mL (0.5:1) showed an increase in surface charge towards more negative as the ratio of DS was increased. This negative charge could only arise from the excess DS adsorbed on the surface of particles. On the other hand, increase in size was observed when peptide was incorporated, suggesting that peptide has formed close association with nanoparticle matrix material. The charge of peptide-loaded nanoparticles, changed from positive to negative as the ratio of the DS in the formulation increased, leads one to believe that almost all the ARH peptide might have been incorporated into the nanoparticles. But these speculations are not supported

by the ARH peptide loading and entrapment efficiency data. It is possible that some ARH peptide formed soluble ionic complex with DS as ARH is a fairly small molecule (Mw 927).

Figure 23: Linear profile exhibited by low concentration of ARH peptide standards by fluorimetry assay method.

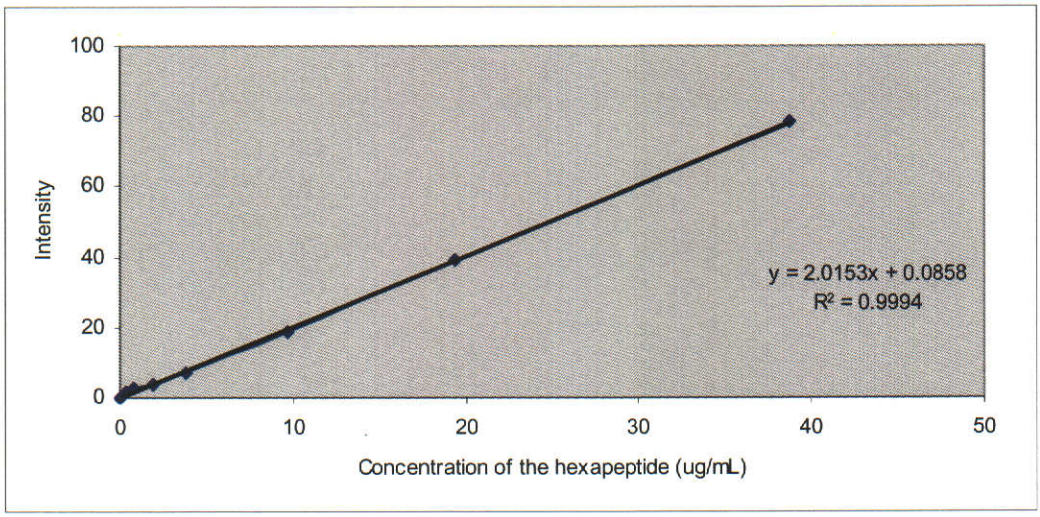

Table 9: Influence of the ratio of matrix materials (CS/DS) on the physico-chemical characteristics of empty and ARH peptide loaded nanoparticles.

Sample	CS/DS ratio	pH of the preparation	Size (nm)*	Zeta Potential (mV)
Empty	5mL:5mL (1:1)	3.67	553 ± 10	-22.0
Loaded	5mL:5mL (1:1)	3.68	867 ± 50	43.9
Empty	5mL:8.5mL (0.59:1)	3.96	222 ± 15	-32.6
Loaded	5mL:8.5mL (0.59:1)	3.95	257 ± 5	-8.7
Empty	5mL:10mL (0.5:1)	3.64	219 ± 2	-34.3
Loaded	5mL:10mL (0.5:1)	3.68	247 ± 25	-32.1

*Size measurement data are the average value of three measurements ± one standard deviation. (n=3)

Figure 24: Particle size and Zeta Potential of empty nanoparticles

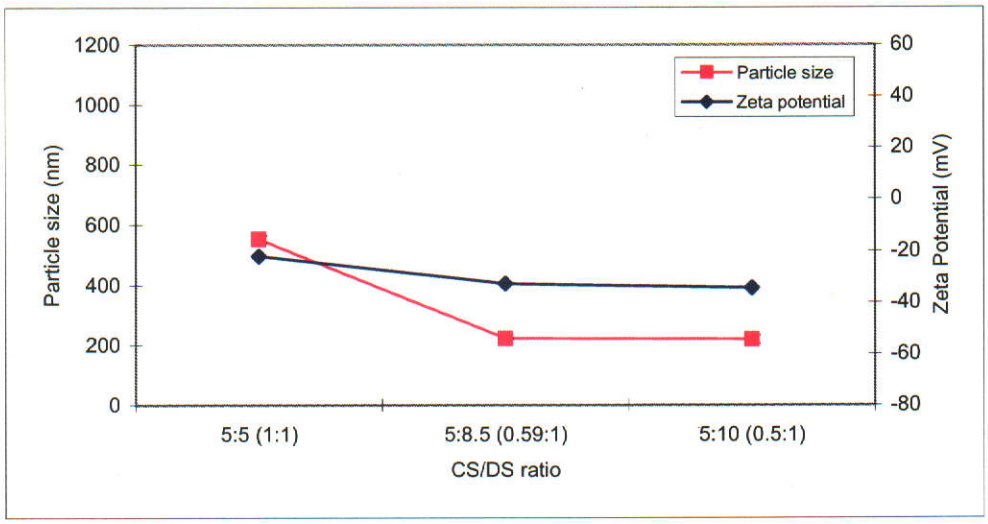

Figure 25: Particle size and Zeta Potential of ARH peptide-loaded nanoparticles.

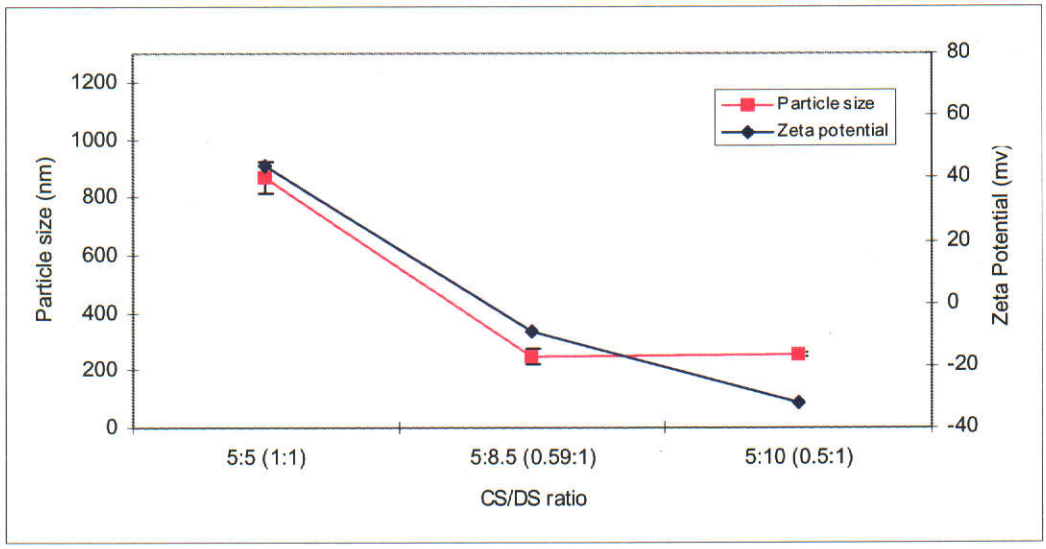

3.4.2 Morphology of ARH peptide-loaded nanoparticles

TEM images of peptide-loaded CS/DS nanoparticles prepared from 5mL:8.5mL (0.59:1) ratio are shown in the Figure 26 and 27. It is seen that these particles exhibited a solid

structure but different from that of BSA-loaded nanoparticles in shape. They appear to be less smooth and less spherical.

Figure 26: Transmission electron micrograph of ARH peptide loaded CS/DS nanoparticle system with CS/DS ratio of 5mL : 8.5 mL (0.59:1).

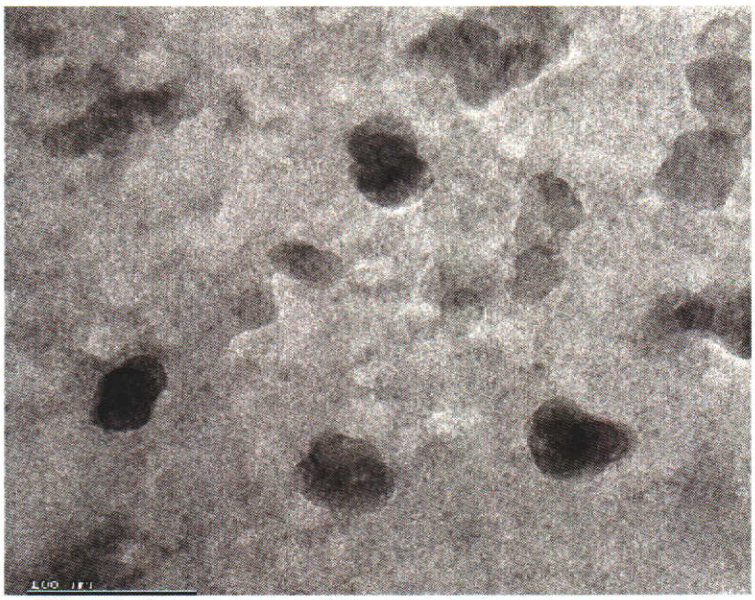

100nm Scale

Figure 27: Transmission electron micrograph of ARH peptide loaded CS/DS nanoparticle system with CS/DS ratio of 5mL : 8.5 mL (0.59:1).

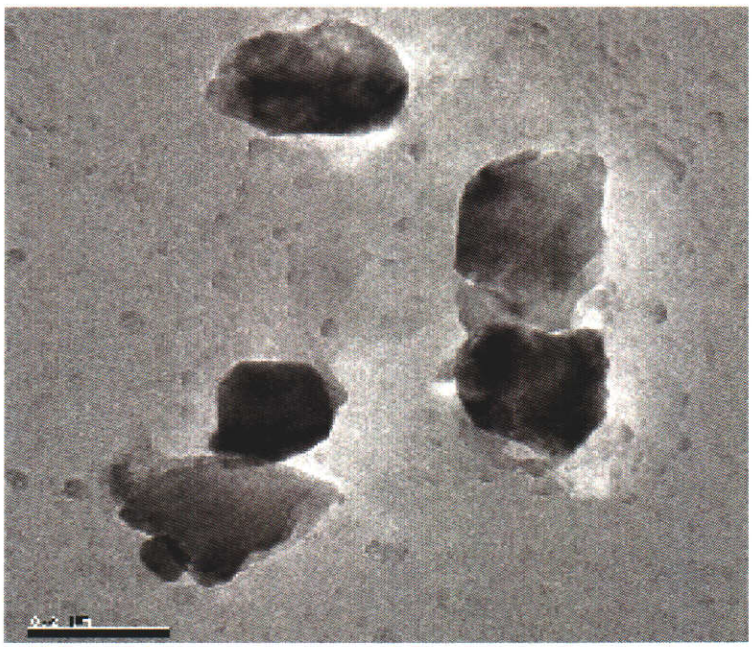

500nm Scale

3.4.3 Loading and entrapment efficiency

Effect of ratio of CS/DS on nanoparticles loading and entrapment efficiency of peptide is presented in Table 10 and Figure 28. The loading capacity of peptide for 5mL:5mL (1:1) and 5mL:8.5mL (0.59:1) CS/DS nanoparticles ratios is 12.3% w/w and 13.4% w/w respectively, with entrapment efficiency of 72.9% w/w and 75.9%w/w. These results were different from those obtained in the BSA study. Based on the BSA study, one would expect the higher the concentration of DS, the higher the encapsulation efficiency. In fact this hypothesis failed in the case of 5mL:10mL (0.5:1) CS/DS ratio. The loading capacity as well as entrapment efficiency (10.9% w/w and 36.3% w/w respectively) of 5mL:10mL (0.5:1) ratio nanoparticles is lower than the other two ratios studied, despite the fact that a larger amount of DS was used. It is speculated that this decrease in loading level might be due to the smaller initial amount of ARH peptide added to DS solution, resulting in lower theoretical loading as expected. However, the much lower entrapment efficiency (36.3% w/w) is unexpected. The duplicate preparation confirmed this level (Table 11), suggesting factors other than experimental error may be the cause. One possible explanation is the formation of soluble ionic complex between ARH peptide and DS.

It can be noted from the results in Table 10 that there is no clear trend between the CS/DS ratio and entrapment efficiency. Though the maximum entrapment efficiency 75.9% w/w was obtained with 5mL:8.5mL (0.59:1) ratio of CS/DS nanoparticles, this level is much lower when compared to the BSA study which achieved 100% w/w with the same

formulation. When the loading and loading efficiency of ARH peptide (Table 10) was compared with that of BSA study (Table 8), it can be seen the actual loading of peptide appeared much lower than that of BSA, largely due to a smaller amount of ARH peptide added (only about half of BSA quantity was used) to the starting DS solution. The loading efficiency, however, is consistently at 80 to 81% level, suggesting the actual loading is affected more by the initial amount of ARH peptide in DS solution, rather than CS/DS ratio, which is contrary to what is seen with BSA incorporation into nanoparticles. It is suspected that the huge difference in the molecular size of BSA and ARH peptide may have an impact on the incorporation. The molecular size of BSA (Mw 60,000) is much larger than that of ARH peptide whose molecular weight is only 927, and these small molecules could have readily diffused out through the polymer matrix of nanoparticles to establish the equilibrium and also form soluble ionic complex with DS. This in turn could have resulted in a low ARH peptide loading.

Pan et al. reported the insulin loading capacity and their association efficiency were affected by concentration of insulin in the opposite charged polyanion tripoly- phosphate and the amount of insulin added (70), with increasing ratio of insulin to CS resulted in slight decrease of entrapment efficiency but a great increase in loading capacity. In our case 5mL:5mL (1:1) and 5mL:8.5mL (0.59:1) ratios showed slight higher loading and entrapment efficiency compared to that of 5mL:10mL (0.5:1). This might be due to relatively higher initial concentration of ARH peptide (0.32mg mL^{-1}) in DS solution with the two ratios. On the other hand only 0.27mg mL^{-1} ARH peptide in DS solution was used with 5mL:10mL (0.5:1) ratio, despite the final concentration of ARH peptide in the

CS/DS mixture was very similar (0.20 and 0.18mg mL^{-1} respectively). This suggests that for the 5mL:10mL (0.5:1) CS/DS ratio, the loading capacity and entrapment efficiency, may be affected by the initial concentration of ARH peptide in the DS solution. It could be more comparable if the initial level of ARH peptide concentration was kept the same. Due to high cost and availability of ARH peptide, we had to modify the quantity in the study. Hence, further studies are required to confirm this speculation.

Table 10: Influence of the ratio of matrix materials (CS/DS) on the drug loading and entrapment efficiency of ARH peptide-loaded nanoparticles.

CS/DS ratio	Loading (%)		Entrapment efficiency (%)	pH of CS solution	pH of DS solution	Yield (%)
	Theoretical	Actual				
5mL:5mL (1:1)	15.3	12.3 (80.4%)*	72.9	3.56	4.86	84.6
5mL:8.5mL (0.59:1)	16.7	13.4 (80.2%)*	75.9	3.62	4.84	94.2
5mL:10mL (0.5:1)	13.42	10.9 (81.2%)*	36.3	3.53	4.85	50.8

* Values in bracket are the loading efficiency as per definition in Table 8.

Figure 28: Effect of ratio of matrix materials (CS/DS) on ARH peptide loading and entrapment efficiency.

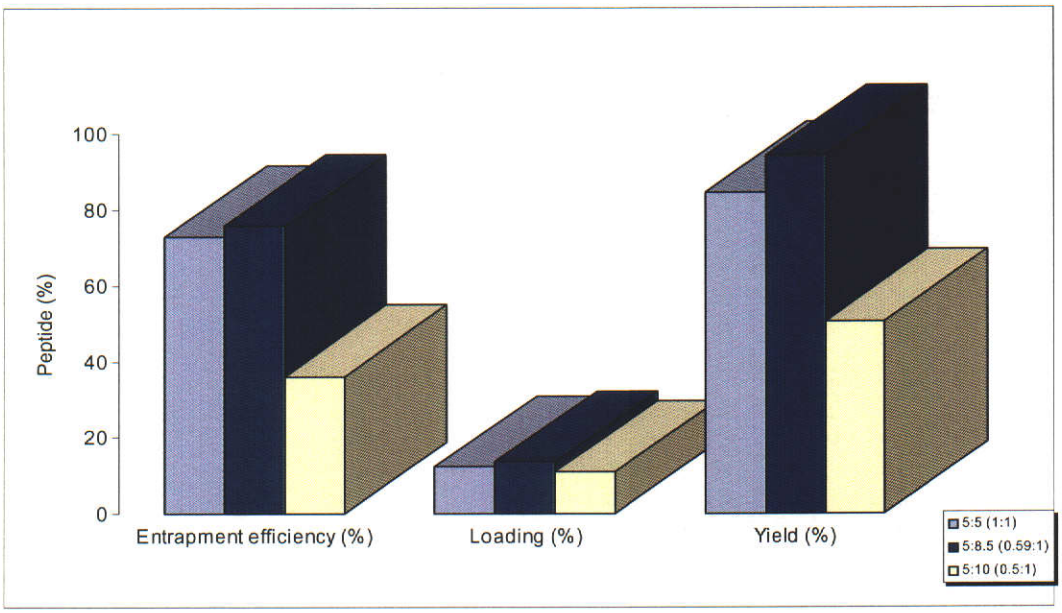

Table 11: Comparing the two batches of ARH peptide loaded 5:10 (0.5:1) ratio of CS/DS nanoparticles.

Sample	**CS/DS ratio**	**Size (nm)**	**Zeta Potential (mV)**	**Loading (%)**	**Entrapment efficiency (%)**	**Yield (%)**
A	5mL:10mL (0.5:1)	248± 28	-32.1	10.9	36.2	50.8
B	5mL:10mL (0.5:1)	237± 7	-32.6	ND	40.5	ND

ND: Not done due to the lack of sufficient sample.

3.4.4 *In-vitro* release of ARH peptide from CS/DS nanoparticles

ARH peptide nanoparticles, prepared under the experimental conditions described in Table 8 and 9, were evaluated for *in vitro* peptide release at 37°C. Figure 29, 30, 31, 32, 33, 34, 35, 36, 37 and 38 show the plot of the release data expressed as cumulative percentage as well as differential release of ARH peptide *in vitro* from the CS/DS nanoparticles against time.

In most cases, the peptide appeared to be released in a biphasic fashion, characterized by an initial rapid release period followed by continuously slower release. Different levels of initial release or burst effect were observed for different ratios of CS/DS nanoparticles (Figure 36) in10mM phosphate buffer pH 7.4, which is different from the results obtained from the initial BSA study.

Figure 29: Cumulative release of ARH peptide from nanoparticles prepared by mixing 5ml of 0.1% w/v CS with 5ml of 0.1% w/v DS, CS/DS ratio 5mL: 5mL (1:1); Loading 12.3% w/w.

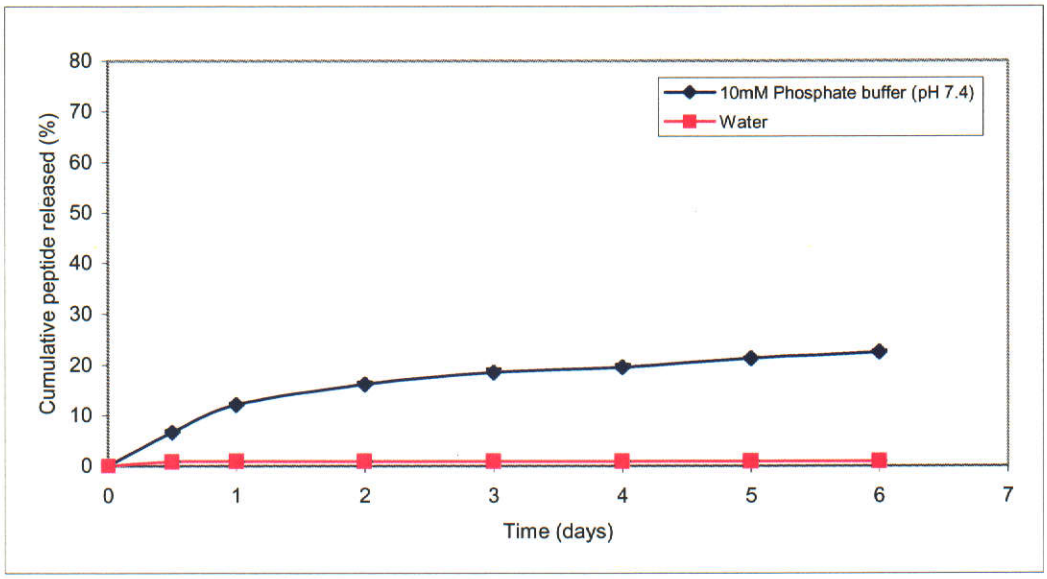

Figure 30: Differential release of ARH peptide from nanoparticles prepared by mixing 5ml of 0.1% w/v CS with 5ml of 0.1% w/v DS, CS/DS ratio 5mL: 5mL (1:1); Loading 12.3% w/w.

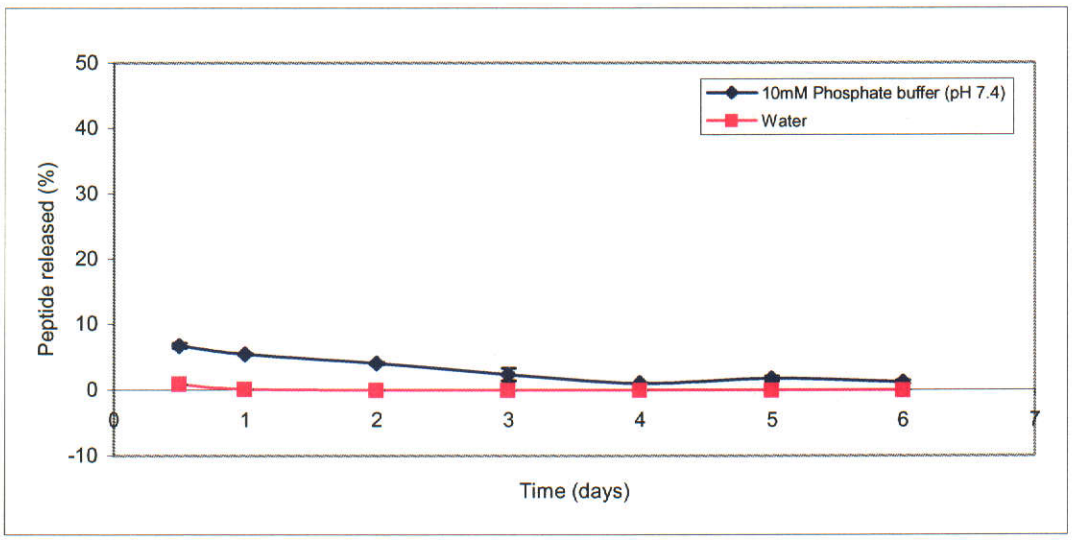

Figure 31: Cumulative release of ARH peptide from nanoparticles prepared by mixing 5ml of 0.1% w/v CS with 8.5ml of 0.1% w/v DS, CS/DS ratio 5mL: 8.5mL (0.59:1); Loading 13.4% w/w.

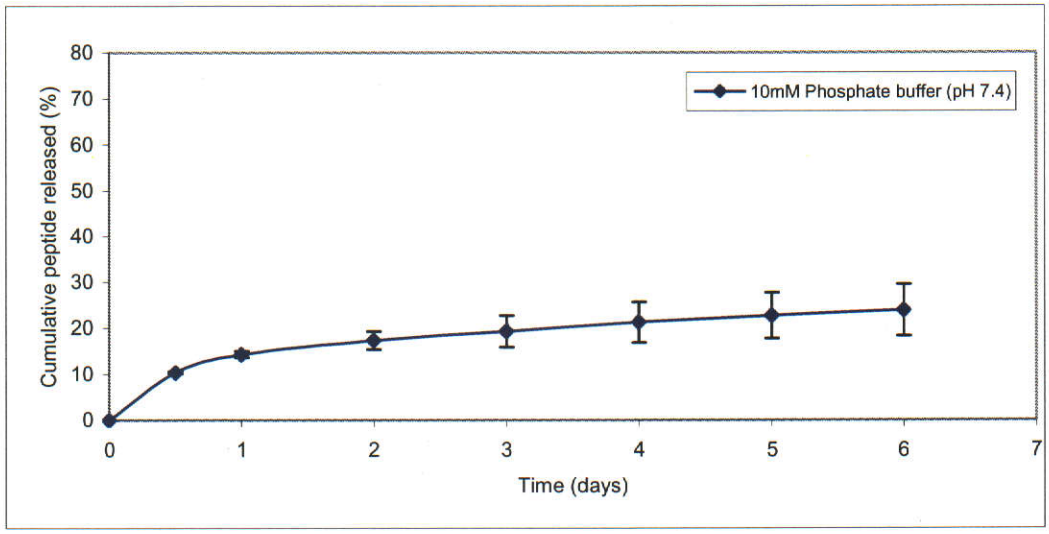

Figure 32: Differential release of ARH peptide from nanoparticles prepared by mixing 5ml of 0.1% w/v CS with 8.5ml of 0.1% w/v DS, CS/DS ratio 5mL: 8.5mL (0.59:1); Loading 13.4% w/w.

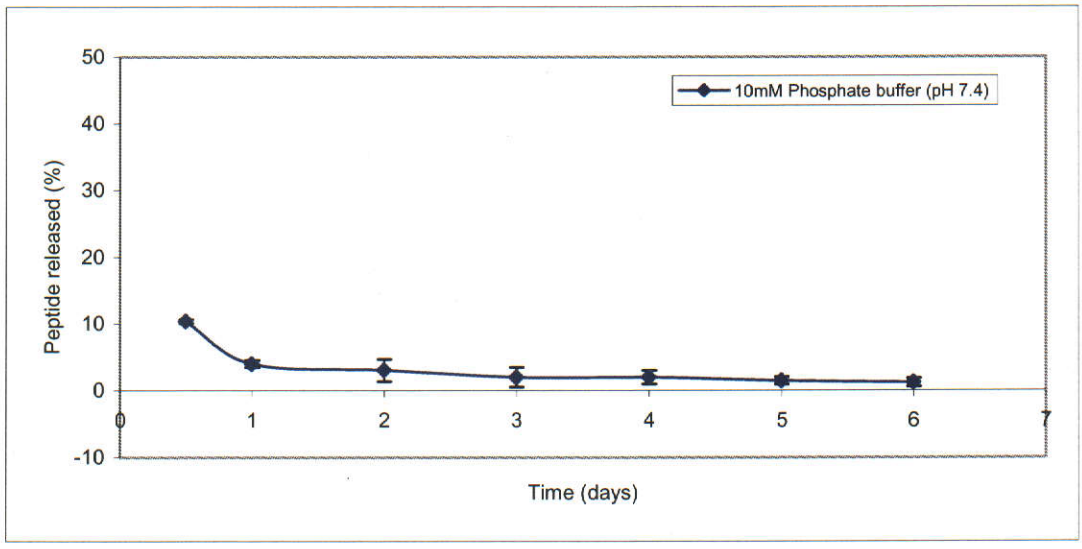

Figure 33: Cumulative release of ARH peptide from nanoparticles prepared by mixing 5ml of 0.1% w/v CS with 10ml of 0.1% w/v DS, CS/DS ratio 5mL: 10mL (0.5:1). Loading 10.9% w/w.

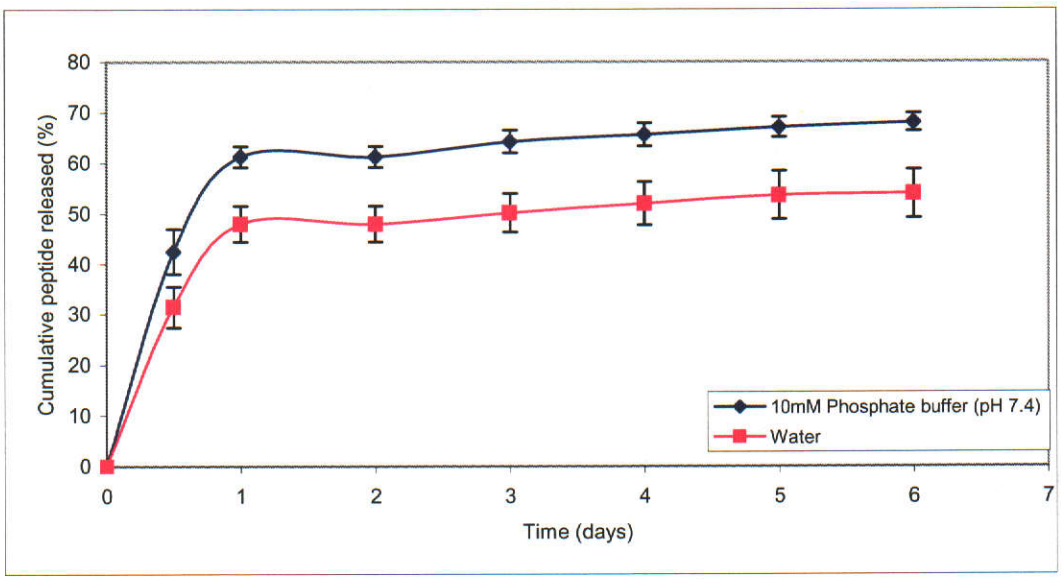

Figure 34: Differential release of ARH peptide from nanoparticles prepared by mixing 5ml of 0.1% w/v CS with 10ml of 0.1% w/v DS, CS/DS ratio 5mL: 10mL (0.5:1); Loading 10.9% w/w.

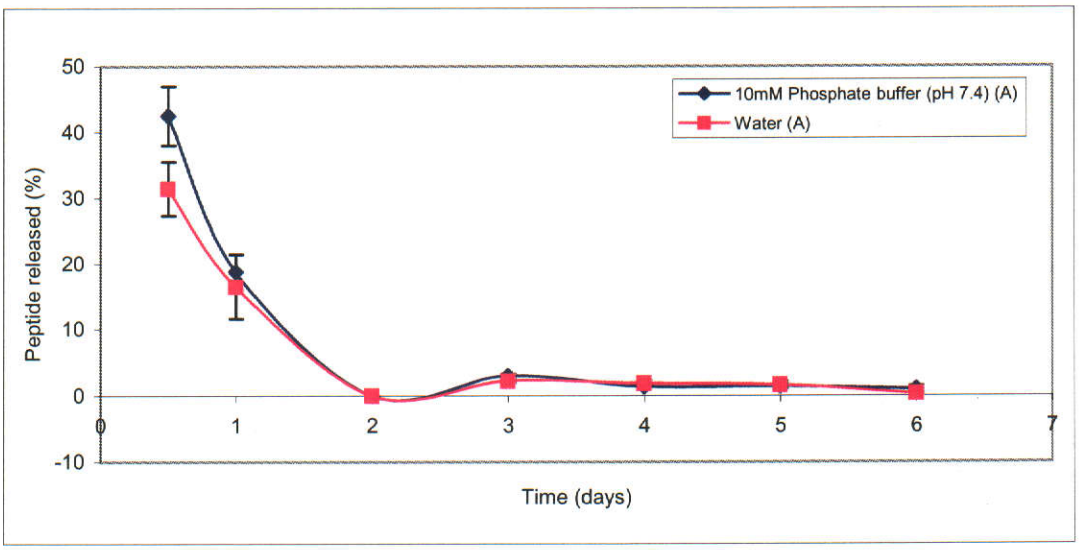

Figure 35: Cumulative release of ARH peptide loaded CS/DS nanoparticles in 10mM phosphate buffer (pH 7.4).

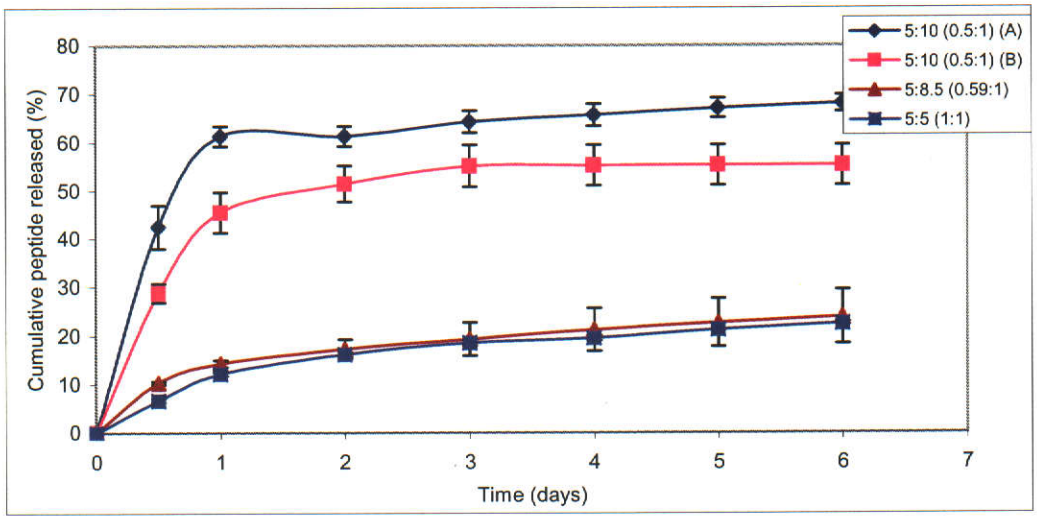

Figure 36: Differential release of ARH peptide loaded CS/DS nanoparticles in 10mM phosphate buffer (pH 7.4).

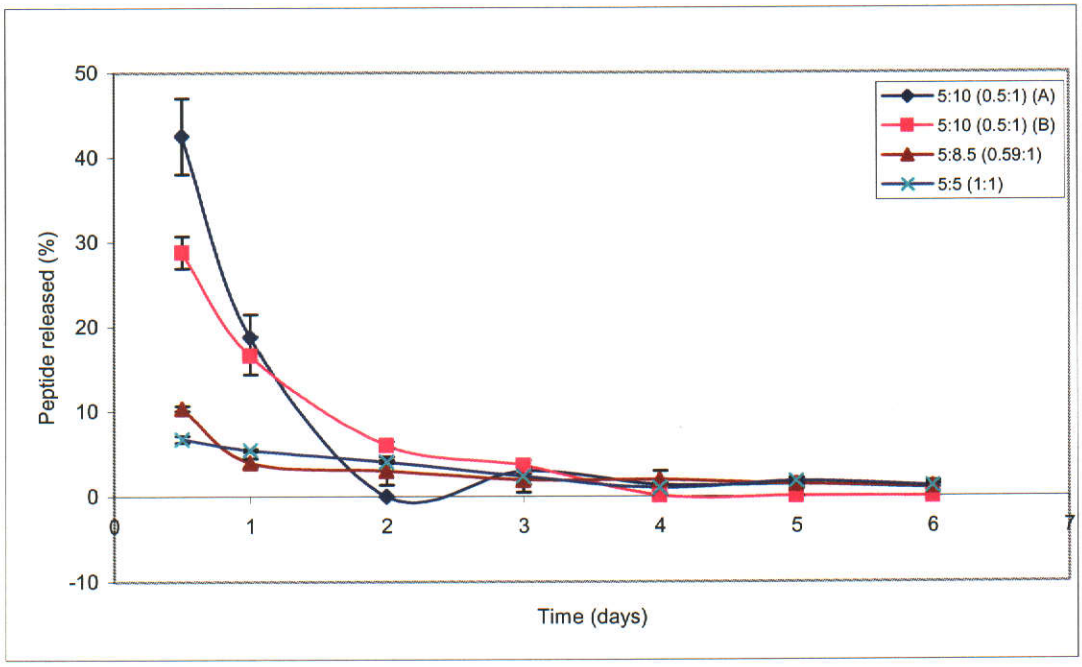

Figure 37: Cumulative release of ARH peptide loaded CS/DS nanoparticles in water.

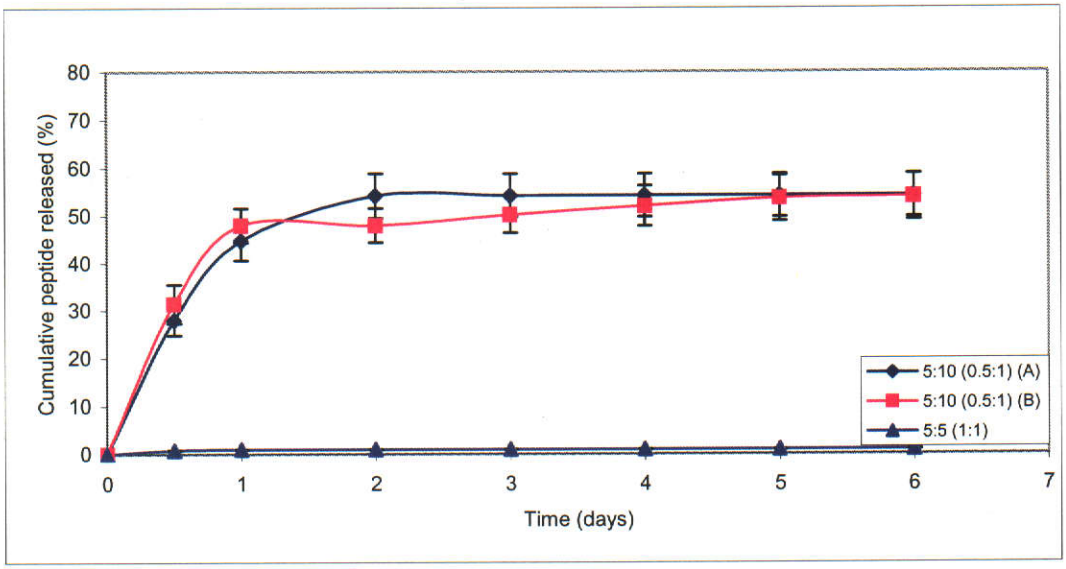

Figure 38: Differential release of ARH peptide loaded CS/DS nanoparticles in water.

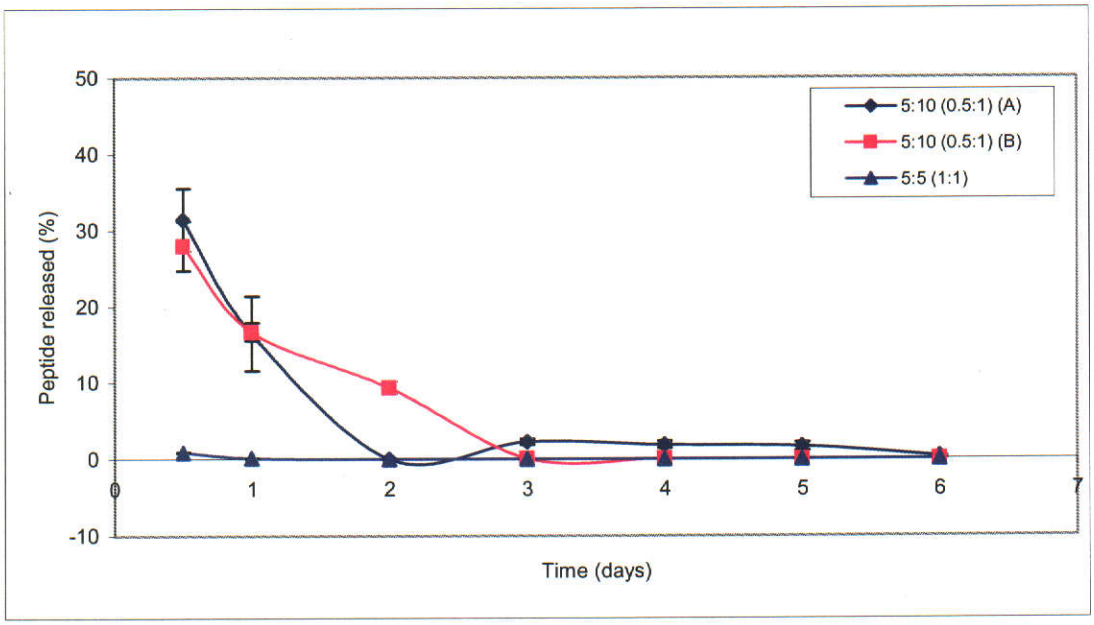

On the other hand, when deionised water was used as the release media, 5mL:5mL (1:1) CS/DS ratio nanoparticles showed a level of release less than 10% in 7 days, which was consistent with the BSA study results, whereas, 5mL:10mL (0.5:1) ratio CS/DS nanoparticles exhibited an initial burst release of 28% peptide release in 12 hours (Figure 37 and 38). After this initial release, the ARH peptide was released in a much lower level for up to 7 days reaching percentage of cumulative release close to 58% for 5mL:10mL (0.5:1). The same trend is also seen in the buffered media. This is in total contrast to the initial BSA study, which showed a very much lower level of BSA release in water than that in buffered media. This finding suggests disassociation of peptide from CS/DS nanoparticles may not be controlled by ion-exchange process.

In 10mM phosphate buffer pH 7.4, the ARH peptide released at various rates from the three different ratios of CS/DS nanoparticles (Figure 35 and 36): 22%, 23% and 68% of ARH peptide released in 7 days by 5mL:5mL (1:1), 5mL:8.5mL (0.59:1), and 5mL:10mL (0.5:1) ratio CS/DS nanoparticles respectively. It demonstrates the higher the ratio of DS in the formulation, the faster the release of peptide from the nanoparticles, which is contrary to the findings in the BSA study. From the initial BSA study, we noted that the higher the DS ratio, the slower the release of BSA in buffered media. However, the ARH peptide-loaded nanoparticles prepared from the 5mL:10mL (0.5:1) ratio of CS/DS produced an unexpected result. To confirm the finding, a separate batch of nanoparticle formulation was prepared using 5mL:10mL (0.5:1) ratio and its release was assessed. The results obtained are the same.

It appears that factors other than experimental error may be the cause. We speculate that the release behavior of the three types of nanoparticulate formulation might be influenced by their particle size, zeta potential and its related high dispersibility and stability of nanoparticles. From Table 9, it can be seen that an increase in concentration of the DS results in a decrease in size of the nanoparticles and an increase in magnitude of zeta potential. It is well known that the small size of nanoparticles has a major influence on the release rate (40). These particles have a high surface area per volume; therefore most of the peptide will be at or near the particle surface and can be readily released. Furthermore, the diffusion distances encountered in the particles are small which allows drug trapped in the core to rapidly diffuse out and also for the release medium to diffuse in. Comparing the system of 5mL:10mL (0.5:1) with that of 5mL:8.5mL (0.59:1), although both showed equivalent particle size, the latter did have a much smaller zeta potential. This suggest that the nanoparticles of 5mL:8.5mL (0.59:1) ratio of CS/DS may not be very stable as a dispersion and have a high tendency to coagulate, therefore increasing particle size. Indeed, it was noticed that the system of 5mL:10mL (0.5:1) ratio is more readily dispersed whereas the system of 5mL:8.5mL (0.59:1) tends to aggregate during the study.

4. Conclusions

In this research project we have developed a novel biodegradable nanoparticle system solely made of hydrophilic polymers, i.e. CS and DS, for the delivery of BSA and ARH peptide. Major advantages of this nanoparticle technology include that the process is very simple, and nanoparticles can be prepared in a short time and under extremely mild conditions with ionic cross-linkage, without involving high temperatures or sonication. The physicochemical characterization of these nanoparticles revealed that the particle size and surface charge are dependent on the CS and DS concentration and ratio. They can be modulated by varying the ratio of two ionic polymers. A high loading capacity and a continuous release of a protein over extended periods of time can be achieved readily. For the small molecule ARH peptide, a reasonable incorporation with entrapment efficiency of 75% was also achieved with the optimum CS/DS ratio being 5mL:5mL (1:1) to 5mL:8.5mL (0.59:1). The release of BSA from the nanoparticles was slow and relatively constant, whereas, ARH peptide showed a similar slow release with 5mL:5mL (1:1) and 5mL:8.5mL (0.59:1) ratio nanoparticles but at high DS ratio of 5mL:10mL (0.5:1) the release was in a biphasic fashion with an initial large burst release followed by a very slow rate up to 7 days in 10mM phosphate buffer pH 7.4. It was found that the slow release of BSA was correlated to the high DS ratio in nanoparticles formulation, whereas, the ARH peptide only showed the slow release at CS/DS ratio of 5mL:5mL (1:1) and 5mL:8.5mL (0.59:1) but not 5mL:10mL (0.5:1). The differences observed with BSA and ARH peptide release behavior could be possibly due to the differences in their molecular size, their entanglement with polymer matrix structure and solubility of ionic complex formed.

A better understanding of the release mechanism of proteins and peptides from these CS/DS nanoparticles obviously is required in the future study. This will provide a basis for their further optimization, thus opening more exciting opportunities for improving the administration of Biomolecules. But all other interesting features render this novel nanoparticle system as a very promising vehicle for the formulation of therapeutic proteins and peptides.

This research project has completed the following work

(1) Developed a simple and effective method to formulate biodegradable nanoparticles for the delivery of the model protein BSA and an ARH peptide.

(2) Investigated major factors, which determined nanoparticle formation and incorporation of the protein and the peptide.

(3) Studied underlying mechanisms controlling their incorporation and release characteristics.

Still there are many questions arising from this study remain to be answered in the future. These include the confirmation of presence of soluble ionic complex formed by ARH peptide and DS; the stability of protein and peptide in the nanoparticle formulation; finally the biological activities of protein and peptide-loaded nanoparticles.

5. References

1. Silverberg E, Boring CC, Squires TS. Cancer statistics. CA. Cancer. J. Clin. 1990;40:9-26.

2. Liotta LA, Steeg PS, Stevenson WG. Cancer metastasis and angiogenesis: an imalance of positive and negative regulation. Cell 1991; 64:327.

3. Fife RS, Sledge GW, Sissons S, Zerler B. Effects of tetracyclines on angiogenesis in vitro. Cancer Lett. 2000;153:75-78.

4. Bussolino F, Mantovani A, Persico P. Molecular mechanism of blood vessel formation. Trends. Biochem. Sci. 1997;22:251-256.

5. Bae DG, Gho YS, Yoon WH, Chae CB. Arginine-rich anti-vascular endothelial growth factor peptides inhibit tumor growth and metastasis by blocking angiogenesis. J. Biochem 2000;275:13588-13596.

6. Bodmeier R, McGinity JW. Solvent selection in the preparation of poly (DL-Lactide) microspheres prepared by the solvent evaporation method. Int. J. Pharm. 1988;43:179-186.

7. Couvreur P, Puiseux F. Nano- and microparticles for the delivery of peptides and proteins. Adv. Drug Deliv. Rev. 1993; 5: 141-162.

8. Zimmer A, Kreuter J. Microspheres and nanoparticles used in ocular drug delivery systems. Adv. Drug. Deliv. Rev. 1995;16:61-73.

9. Amiji M, Park K, Shalaby SW, Ikada Y, Langer R, Williams J. Polymers of biological significance. ACS Symp. Ser. 540, Washington, DC. 1994.

10. Calvo P, Vila-Jato JL, Alonso MJ. Comparitive in vitro evaluation of several colloidal systems, nanoparticles, nanocapsules and nanoemulsions as ocular drug carriers. J. Pharm. Sci. 1996;85:530-536.

11. Brigger I, Dubernet C, Couvreur P. Nanoparticles in cancer therapy and diagnosis. Adv. Drug. Del. Rev. 2002;54:631-651.

12. Widder KJ, Senyei AE, Ranney DF. Magnetically responsive microspheres and other carriers for the biophysical targeting of antitumour agents. Adv. Pharmacol. Chemother. 1979;16:213-271.

13. Cummings J. Microspheres as a drug delivery system in cancer therapy. Exp. Opin. Ther. Patents 1998;8:153-171.

14. Welling PG, Patel RB, Patel RU, Gillespie WR, Craigo WA, Albert KS. Bioavailability of tolazamide from tablets: Comparision of in vitro and in vivo results. J. Pharm. Sci 1982;71:1259-1263.

15. Cowsar DR. Introduction to controlled release, in: A.C.Tanquary and R.E.Lacey (eds). Control. Rel. Bio. Act. Agents. 1979:Plenum Press, New York.

16. Chen Y. In vitro characterisation and in vivo evaluation of microspheres as carriers for the anti-cancer drug adriamycin. Ph.D Thesis. 1989:University of Strathclyde, Glasgow.

17. Law SL, Lo WY, Teh GW. The leakage characteristics of liposome encapsulated adriamycin-dextran conjugates. Drug Dev. Ind. Pharm. 1988;14:143-153.

18. Gallo JM, Hassan EE. Receptor-mediated magnetic carriers: basis for targeting. Pharm. Res. 1988;5:300-403.

19. Couvreur P, Gruslain L, Lenaerts V, Brasseur F, Guiot P. Polymeric nanoparticles and microspheres. Boca Raton, Florida: CRC Press; 1986.

20. Esposito E, Cortesi R, Cervellati F, Menegatti E, Nastruzzi C. Biodegradable microparticles for sustained delivery of tetracycline to the periodontal pocket: formulatory and drug release studies. J. Microencapsulation. 1997;14:175-187.

21. Kreuter J. Nanoparticles. In: J. Kreuter, Editor, Colloidal drug delivery systems. New York: Marcel Dekker; 1994: 219-342.

22. Zambaux MF, Bonneaux F, Gref R, Maincent P, Dellacherie E, Alonso MJ, et al. Influence of experimental parameters on the characteristics of poly (lactic acid) nanoparticles prepared by a double emulsion method. J. Control. Rel. 1998;50:31-40.

23. Niwa T, Takeuchi H, Hino T, Kunou N, Kawashima Y. Preparations of biodegradable nanospheres of water-soluble an dinsoluble drugs with D, L- lactide/glycolide copolymer by a novel spontaneous emulsification solvent diffusion method and drug release behaviour. J. Control. Rel 1993;25:89-98.

24. Tom JW, Debenedetti PG. Formation of bioerodiable polymeric microspheres and microparticles by rapid expansion of supercritical solution. Biotechnol. Prog. 1991;7:403-411.

25. Tom JW, Debenedetti PG, Jerome R. Preparation of poly (L0lactic acid) and composite poly (L-lactic acid)-pyrene by rapid expansion of supercritical solution. J. Supercrit. Fluids. 1994;7:9-29.

26. Randolph TW, Randolph AD, Mebes M, Yeung S. Sub-micron-sized biodegradable particles of poly (L-lactic acid) via the gas antisolvent spray precipitation process. Biotechnol. Prog. 1993;9:429-435.

27. Couvreur P, Kante B, Roland M, goit P, Bauduin P, Speiser P. Polycyanoacrylate nanocapsules as potential lysosomotropic carriers: Preparation, morphology and sorptive properties. J. Pharm. Pharmcol. 1979;31:331-332.

28. Calvo P, Remunan-Lopez C, Vila-Jato JL, Alonso MJ. Chitosan and chitosan/ethylene oxide-propylene oxide block copolymer nanoparticles as novel carriers for proteins and vaccines. Pharm. Res. 1997;14:1431-1436.

29. Calvo P, Remunan-Lopez C, Vila-Jato JL, Alonso MJ. Novel hydrophilic chitosan-polyethylene oxide nanoparticles as protein carriers. J. Appl. Polym. Sci. 1997;63:125-132.

30. Shu XZ, Zhu KJ. The influence of multivalent phosphate structure onthe properties of ionically cross-linked chitosan films for controlled drug release. Eur. J. Pharm. Biopharm. 2002;54`:235-243.

31. Calvo P, Vila-Jato JL, Alonso MJ. Approaches to improve the association of amikacin sulfate to poly (cyanoacrylate)nanoparticles. Int. J. Pharm 1991;68:69-79.

32. Yoo HS, Oh JE, Lee KH, Park TG. Biodegradable nanoparticles containing doxorobucin-PLGA conjugate for sustained release. Pharm. Res. 1999;16:1114-1118.

33. Janes KA, Calvo P, Alonso MJ. Polysaccharide colloidal particles as delivery systems for macromolecules. Adv. Drug. Deliv. Rev. 2001;47:83-97.

34. Washington C. Drug release from microdisperse systems. Int. J. Pharm 1990;58:1-12.

35. Muller H, Willis KM. Surface modification of i.v.injectable biodegradable nanoparticles with poloxamer polymers and poloxamine 908. Int. J. Pharm. 1993;89:25-31.

36. Jalil R, Nixon JR. Biodegradable poly (lactic acid) and poly (lactide-co-glycolide) microcapsules: problems associated with preparative techniques and release properties. J. Microencapsul. 1990;7:297-325.

37. Fresta M, Puglisi G, Giammona G, Cavallaro G, Micali N, Furneri PM. Pefloxacin mesilate and ofloxacin-loaded polyethylcyanoacrylate nanoparticles; characterisation of the colloidal drug carrier formulation. J. Pharm. Sci 1995;84:895-901.

38. Polakovic M, Gorner T, Gref R, Dellacherie E. Lidocaine loaded biodegradable nanoparticles. II.modelling of drug release. J. Control. Rel. 1999;60:169-177.

39. Nishioka Y, Yoshino H. Lymphatic targeting with nanoparticulate system. Adv. Drug. Deliv. Rev. 2001;47:55-64.

40. Redhead HM, Davis SS, Illum L. Drug delivery in poly (lactide-co-glycolide) nanoparticles surface modified with poloxamer 407 and poloxamine 908: in vitro characterisation and in vivo evaluation. J. Control. Rel. 2001;70:353-363.

41. Jani P, Halbert GW, Langridge J, Florence T. The uptake and translocation of latex nanospheres and microspheres after oral administration to rats. J. Pharm. Pharmcol. 1989;41:809-812.

42. Mathiowitz E, Jacob JS, Jong YS, Carino GP, Chickering DE, Chaturvedi P, et al. Biologically erodable microspheres as potential oral drug delivery systems. Nature. 1997;386:410-414.

43. Ratner BD, Johnston AB, Lenk TJ. Biomaterial surface. J. Biomed. Mat. Res. 1987;21:59-90.

44. Carstensen H, Muller BW, Muller RH. Adsorption of ethoxylated surfactants on nanoparticles. I. Characterisation by hydrophilic interaction chromatography. Int. J. Pharm. 1991;67:29-37.

45. Ravikumar MNV. A review of chitin and chitosan applications. React. Funct. Polym. 2000;46:1-27.

46. Couvreur P, Puiseux F. Nano- and microparticles for the delivery of peptides and proteins. Adv. Drug Deliv. Rev. 1993;5:141-162.

47. Kawashima Y. Nanoparticulate systems for improved drug delivery. Adv. Drug. Deliv. Rev. 2001;47:1-2.

48. Gulyaev AE, Gelperina SE, Skidan IN, Antropov AS, Kivman GY, Kreuter J. Significant transport of doxorubicin into the brain with polysorbate 80-coated nanoparticles. Pharm. Res. 1999;16:1564-1569.

49. Schipper NGM, Varum KM, Artursson P. Chitosan as absorption enhancers for poorly absorbable drugs 1: Influence of molecular weight and degrre of acetylation on drug transport across human intestinal epithelia (Caco-29 cells). Pharm. Res. 1996;13:1686-1692.

50. Chandra R, Rustgi R. Biodegradable polymers. Prog. Polym. Sci. 1998;23:1273-1335.

51. Illum L. Chitosan and its use as a pharmaceutical excipient. Pharm. Res. 1998;15:1326-1361.

52. Dodane V, Vilivalam VD. Pharmaceutical applications of chitosan. Pharm. Sci. Tech. Today. 1998;1:246-253.

53. Lehr CM, Bouwstra JA, Schacht EH, Junginger HE. In vitro evaluation of mucoadhesive properties of chitosan and some other natural polymers. Int. J. Pharm. 1992;78:43-48.

54. Lueben HL, Leeuw BJD, Langemeyer MW, Boer AGD, Verhoef JC, Junginger HE. Mucoadhesive polymers in peroral peptide drug delivery. VI. Carbomer and chitosan improve the intestinal absorption of the peptide buserelin in vivo. Pharm. Res. 1996;13:1668-1672.

55. Illum L, Farraj NF, Davis SS. Chitosan as a novel nasal delivery system for peptide drugs. Pharm. Res. 1994;11:1186-1189.

56. Carreno-Gomez B, Duncan R. Evaluation of the biological properties of soluble chitosan and chitosan microspheres. Proc. 1st Int. Symp. Polym. Ther. London, UK. 1996:74.

57. Carreno-Gomez B, Duncan R. Evaluation of the biological properties of soluble chitosan and chitosan microspheres. Int. J. Pharm. 1997;148:231-240.

58. Cheng CY, Li YK. An aspergillus chitosanase with potential for large -scale preparation of chitosan oligosaccharides. Biotechnol. Appl. Biochem. 2000;32:197-203.

59. Fernandez-Urrusuno R, Remunan-Lopez C, Calvo P, Vila-Jato JL, Alonso MJ. Enhancement of nasal absorption of insulin using chitosan nanoparticles. Pharm. Res. 1999;16:1576-1591.

60. Bodmeier R, Oh K, Pramar Y. Preparation and evaluation of drug containing chitosan beads. Drug Dev. Ind. Pharm. 1989;15:1475-1494.

61. Aspden TJ, Illum L, Skaugrud O. DNA-chitosan nanoparticles for the gene delivery. Proc. Int. Symp. Control. Rel. Bioact. Mater. 1995;22:550.

62. Chen Y, McCulloch RK, Gray BN. Synthesis of albumin-dextran sulfate microspheres possessing favourable loading and release characteristics for the anti-cancer drug doxorubicin. J. Control. Rel. 1994;31:49-54.

63. Bradford M. Arapid and sensitive method for the quantitation of microgram quantities of protein utilizing the principle of protein-dye binding. Anal. Biochem. 1976;72:248-254.

64. Janes KA, Fresneau MP, Marazuela A, Fabra A, Alonso MJ. Chitosan nanoparticles as delivery systems for doxorubicin. J. Control. Rel. 2001;73:255-267.

65. Campos AMD, Sanchez A, Alonso MJ. Chitosan nanoparticles: a new vehicle for the improvent of the delivery of drugs to the ocular surface. Application to cyclosporin A. Int. J. Pharm. 2001;224:159-168.

66. Tekin S, Hensen PJ. Use of the Bradford protein assay in a microtiter plate format. Department of Animal Sciences. University of Florida. 2000.

67. Cabib E, Polacheck I. Protein assay for dilute solution. Methods in Enzymology. 1984;104:318-328.

68. Stoscheck CM. Quantitation of protein. Methods in Enzymology. 1990;182:50-69.

69. Polak TB, Kassai M, Grant KB. A comparision of fluorescamine and napthalene-2,3-dicarboxaldehyde fluorogenic reagents for microplate based detection of amino acids. Anal. Biochem. 2001;297:128-136.

70. Pan Y, Li YJ, Zhao H, Zheng JM, Xu H, Wei G, et al. Bioadhesive polysaccharide in protein delivery system: chitosan nanoparticles improve the intestinal absorption of insulin in vivo. Int. J. Pharm. 2002;249:139-147.

6. Appendix

Appendix –1

Effect of polymer matrix materials (CS and DS) on the Bradford protein assay in the BSA loading study

Sample	Absorbance at 595 nm after reaction with Bradford reagent	
CS/DS ratio	Supernatant of empty nanoparticles	Supernatant of BSA loaded nanoparticles
5:3 (1.67:1)	0.054	0.302
5:5 (1:1)	0.033	0.063
3:5 (0.6:1)	0.037	0.035
5:8.5 (0.59:1)	0.005	0.015

Appendix – 2

Effect of polymer matrix materials (CS and DS) on the Bradford protein assay in the BSA release study

Release Sample of 5:8.5 (0.59:1) ratio CS/DS in water	Absorbance at 595 nm after reaction with Bradford reagent	
Time (day)	Empty nanoparticles	BSA loaded nanoparticles
0.5	0.017	0.024
1	0.016	0.023
2	-0.004	0.003
3	-0.014	-0.001
4	-0.005	-0.009
5	-0.002	-0.005
6	-0.012	-0.006

Release Sample of 5:8.5 (0.59:1) ratio CS/DS in 10mM phosphate buffer pH 7.4	Absorbance at 595 nm after reaction with Bradford reagent	
Time (day)	Empty nanoparticles	BSA loaded nanoparticles
0.5	0.014	0.023
1	0.002	0.011
2	0.006	0.012
3	0.002	0.006
4	-0.010	-0.002
5	-0.004	0.001
6	-0.005	0.002

Appendix – 3

Typical size distribution histogram of nanoparticles